10-4-2019

Stem Cell Based Delivery System in a Non-Regenerative Nail Injury Model

Aundrya Montgomery
aumontgomery@uchc.edu

Stem Cell Based Delivery System in a Non-Regenerative Nail Injury Model

Aundrya Brooke Montgomery

B.S., Alabama State University, 2016

A Thesis

Submitted in Partial Fulfillment of the

Requirements for the Degree of

Master of Science

At the

University of Connecticut

2019

APPROVAL PAGE

Master of Science Thesis

Stem Cell Based Delivery System in a Non-Regenerative Nail Injury Model

Presented by

Aundrya Brooke Montgomery, B.S.

Major Advisor _____
Cato T. Laurencin, M.D., Ph.D.

Associate Advisor _____
Lakshmi Nair, M.Phil., Ph.D.

Associate Advisor _____
Barbara Kream, Ph.D.

Associate Advisor _____
Caroline Dealy, Ph.D.

Associate Advisor _____
Peter Maye, Ph.D.

University of Connecticut

2019

Dedicated to my Auntie

Chaka Montgomery

Acknowledgements

God is great and can do exceedingly and abundantly above all that I can ask or think. Without him I could do nothing, but with him everything is possible. So first, I have to say thank you Lord for everything that you have blessed me with thus far.

"To whom much is given, much is required." There is powerful meaning behind that eight-word quote and I am truly thankful for those who have consistently shown their support for me on my journey thus far. To my family, I could not have done this without you. Mama, Dad, Metres, Granny Shula, Grandaddy Tom, Granny Roda, and Grandaddy Johnny, you all have done an excellent job in raising me into the woman I am today. I couldn't have made it through any of this without any of you.

I would like to thank the Young Innovative Investigator Program and staff and students at the Connecticut Convergence Institute for Translation in Regenerative Engineering. Thank you, Dr. Laurencin, for the opportunity to be a part of your team. The knowledge that I have acquired under your leadership is invaluable and I would like to thank you for preparing me for the road ahead. To my committee members, thank you for your mentorship and assistance throughout my thesis preparation, I am truly grateful.

Coming to UConn Health from Alabama was a life-changing event for me, but looking back on the journey, I wouldn't trade anything for my UConn Health family. I would like to thank my team of mentors that have had a significant impact on my personal life and career path. Drs. Linda Barry, Barbara Kream, Victor Hesselbrock, Kiersten Cates-Kennedy, Caroline Dealy, Granville Wrensford, and Anne Delany and Mrs. Trisha Pitter and Mrs. Lana Angelo, thank you for seeing potential in me when I could not see it myself.

I would like to thank Drs. Eric James and Emmanuel Kuyinu, Mohammed Barajaa, Paulos Mengsteab, Guleid Awale, and Eva Kan for all of your assistance in lab. I would like to especially

thank Dr. Aneesah McClinton for everything, I could not have done this study without you. Last but not least, I would like to thank Dr. Kenyatta Washington for your motivation and assistance with completing my thesis.

List of Abbreviations

Keratin 15	K15
Keratin 14	K14
Involucrin	Ivl
Leucine-Rich Repeat-Containing G Protein Coupled Receptor 6	Lgr6
Aminopeptidase N	*Anpep or* CD13
Keratin 31	K31
Epidermal Growth Factor	EGF
Scanning Electron Microscopy	SEM
Transmission Electron Microscopy	TEM
Glutaraldehyde	GA
1,1,1,3,3,3-Hexafluoro-2-propanol	HFIP
Hexamethyldisilazane	HMDS
Minimum Essential Media	MEM
Fetal bovine serum	FBS
Penicillin/Streptomycin	P/S
Poly(lactide-*co*-glycolide)	PLGA
PLGA-shell; gelatin-core fibers	$Hybrid_1$
Gelatin-shell; PLGA-core fibers	$Hybrid_2$
Uncross-linked	UCL
Cross-linked	CL
Gelatin from Pig Skin, Fluorescein Conjugate	$gelatin^{FITC}$
Phosphate buffered solution	PBS
CellTiter 96® AQ_{ueous} One Solution Cell Proliferation Assay	MTS

List of Figures

List of Figures

List of Tables

Table of Contents

Chapter 1: Introduction

1.1 Clinical Relevance of Nail Regeneration

The human fingertip is an essential component to the hand. It is not only functional – providing sensation for the objects we touch, enabling us to grip items, and perform micro/macro movements – but it also provides aesthetic appeal. The fingernail, or claw in other species, is important for those who like to keep a crisp manicure or simply scratch their back. It provides protection to the fingertip and the underlying nail bed, and most importantly, it can be an indicator of systemic disease.[1]

Thus, acute traumatic injuries to the nail can have an adverse effect on quality of life. The victims of nail injuries – including carpenters who endure fingertip amputations, young children who accidently crush their fingers in car doors, or individuals who tear the nail from its surrounding tissue – all have one thing in common, an uncertain prognosis.[2-4] Depending on the severity of the injury, an individual may or may not regrow a nail that resembles the functional state and cosmetic appearance of the nail prior to injury.[2] Currently, there are no stand-alone treatments for these types of injuries, thus exploring universal techniques and procedures that can be applied in both rural and urban settings is imperative.

Corrective surgeries for nail injuries may result in poor outcomes, including the incorrect phenotype and impaired sensation at the fingertip.[3] The recovery period after surgery averages from weeks to months depending upon the extent of the injury. Personal responsibilities including family needs, employment duties and financial obligations necessitate an expeditious recovery. Therefore, treatments should promote epimorphic regeneration while also time considerate of the recovery process.

Nail splints are used in acute traumatic nail injuries to prevent the fusion of the proximal nail fold and the nail bed tissue.[5] These silicone tools are inserted into the nail root, sutured into the soft tissue to anchor it, and removed up to three weeks later with the regrowth of the nail to follow one to three months later.[6] Materials such as polypropylene prostheses, silicone Inro® Nail splints, and sugar cane biopolymer have been used as nail splints.[7,8] Although polypropylene materials are readily available, the chances of native regeneration remain unknown. Inro® Nail splints are expensive and are not always available when needed. They are more likely to be found in hospitals and doctors' offices with abundant budgets rather than rural areas with limited resources. Currently, there are multiple nail splinting methods that utilize easily accessible materials that are strong enough to protect the recovering nail bed. However, these strategies do not have consistent surgical outcomes and most, excluding the Inro® splints, were not originally designed for assisting nail organ restoration.[8]

An ideal approach to assist with nail organ healing should include regenerative engineering techniques that harness the potential of combining cell biology and biocompatible materials. Whilst nail splinting is dependent upon synthetic, man-made materials at present, future bioengineering strategies ought to improve via the development of cell-based delivery systems to aid with nail regeneration. Establishing a biomimetic cell-delivery system composed of stem cells and a biodegradable substrate could prove useful in stimulating indigenous regeneration while decreasing recovery time and cost, and improving surgical and aesthetic outcomes.

1.2 The Human Hand

The human hand serves as a tool in daily tasks requiring both macro- and micro- movements. Under the control of the somatic nervous system, the hand organ functions in grasping and handling objects as well as serving as a sensor to the body's external environment. The function

of the hand is dependent on the construct of its tissues including bone, ligament, tendon, muscle, and nerves and the relay of information to and from the brain[9]. Twenty-seven bones make up the hands' skeleton and serve to give the organ stability, durability, and work in tandem with other tissues to allow proper movement. The phalanges, finger bones, and the metacarpal bones, found in the palm, function to stabilize and shape the hand.[10] The human fingers extend from the region of the metacarpals, known as the knuckles, and are numbered from one to five, starting with the thumb. The small long bones of the fingers are known as phalanges. There are fourteen phalanges on each hand and their position on each finger is described as proximal, middle, and distal.[10]

Ligaments are tough and flexible fibrous connective tissue that attaches bones together and assists with joining the hand to the wrist.[11] Hand joints, including the interphalangeal and metacarpophalangeal joints, are located between the bones and are surrounded by protective fibrous connective tissue that encapsulates specialized lubricant called synovial fluid.[10] Joints between the knuckles and fingers allow smooth movement needed for proper mechanical function of the hand.

Tendons are responsible for connecting bone to muscle, which is required for the somatic function of the hand. The thenar muscles, hypothenar muscles, interosseous muscles, and lumbricals intrinsically facilitate the movement of the thumb, pinky, and fingers respectively.[12] Extrinsic muscles found in the forearm are connected to the hand via flexor tendons and aid in movements such as bending and extending the fingers.[9] The complexity of the hand includes a network of nerves that are responsible for communicating sensation from the outside environment directly to the brain.[12] The wired connection between the ulnar, radial, and median nerves in the hand to the central nervous system is crucial for differentiating a multitude of stimuli and contributing to the normal function of the hand.[10]

1.3 Human Integument System

The integumentary system, including the skin and all of its appendages, serve as a barrier to protect the body's organs from the outside environment and also aids in regulating internal temperature and other homeostatic processes needed for survival. The skin is the largest organ of the body and works closely with other body systems, such as the circulatory, nervous, and immune systems, to provide an ideal environment required for proper function of cells and other tissues in the body.[10] The integumentary system also includes epidermal appendages such as hair, nails, and various glands that participate in functions similar to that of the skin.[9] The organs of the integumentary system are composed of specific epidermal layers that contribute to their overall function (**Figure 1**). The epidermal layers, stratum basale, stratum spinosum, stratum granulosum, stratum lucideum (only found in the palms of hands and soles of feet), and stratum corneum, consist of various epithelial cell types that are comprised of keratin proteins. The high keratin content of the integument organ is responsible for its mechanical strength and water-resistant properties.[9]

The integument of the hand consists of smooth, pliable skin on the dorsal surface, and tougher, durable skin found on the palm.[10] The skin serves to protect the underlying tissue as well as to enhance the mechanical function of the hand.[9] The tips of fingers contain hard-keratinized structures known as the fingernails, denoted by their shiny appearance.[10]

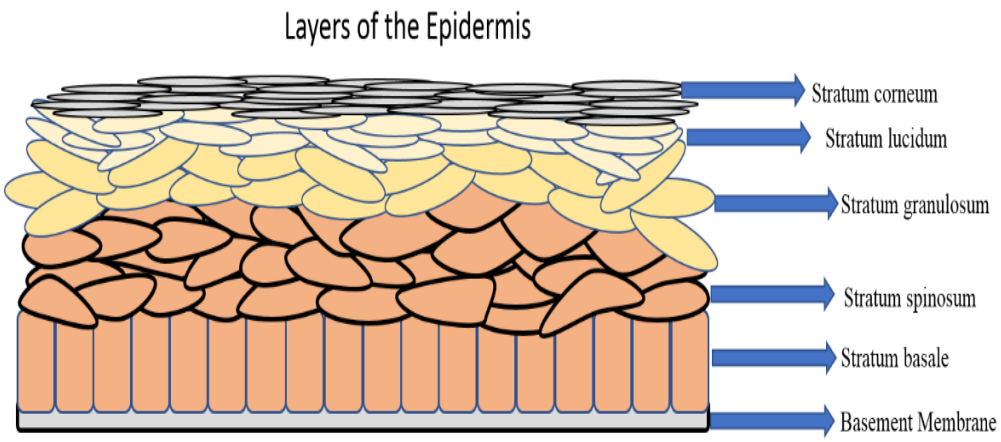

Figure 1. Schematic of epidermal layers found in integument appendages. Illustration by Aundrya B. Montgomery.

1.3.1 The Human Nail

The nail organ protects the fingertip from injury and external pathogens, and aids in the detection of outside stimuli (**Figure 2**). The nail plate inserts beneath the proximal nail fold, and consists of a dorsal roof and ventral floor.[13] It is anchored in place on the fingertip by the lateral nail folds, or paronychium. The eponychium, also known as the cuticle, extends from the proximal nail fold and maintains contact with the dorsal surface of the hard nail plate.[14] The hyponychium is located underneath the distal free edge of hard nail plate and functions in securing the nail to the fingertip. The nail bed, soft tissue found underneath the fingernail, functions as a surface for the nail plate to adhere to during its continuous growth.[15] It is continuous with the nail matrix area comprised of the distal and proximal nail matrix, responsible for supplying the population of cells that ultimately form the nail plate.[16] The lunula, the visual portion of the nail matrix, is identified by its “half-moon” shape and whitish appearance just underneath the nail plate near the cuticle.[15]

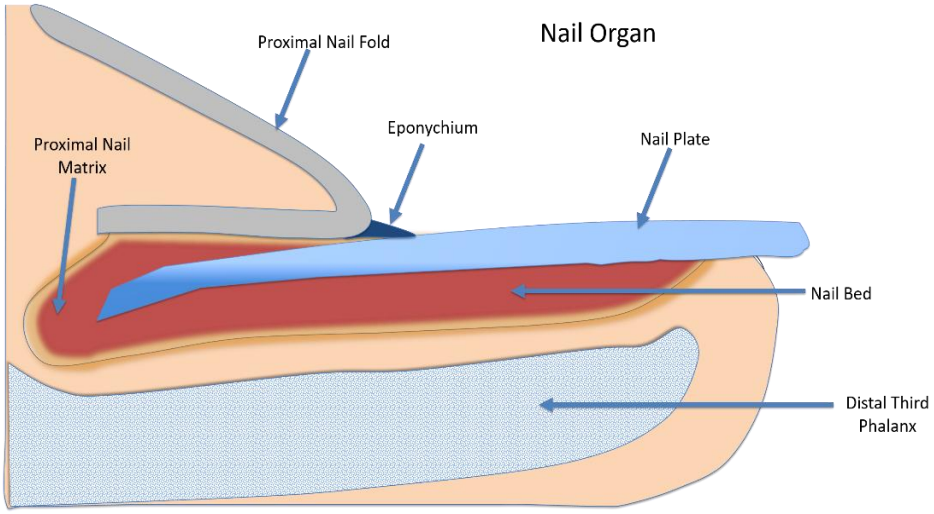

Figure 2. Components of the human nail organ. The human nail consists of the proximal nail fold, proximal nail matrix, eponychium, nail plate, and nail bed. The distal third phalanx is found directly beneath the nail organ.

1.3.2 Human Nail Development

Approximately 10 weeks into gestation, the nail field, recognized by the thickening of the epidermis, appears on the dorsal surface of the fingertips. During this time, the lateral nail folds form and the indentation of the proximal nail fold is noticed to reach to the most proximal end of the third phalanx. Around 20 weeks, keratin fibers begin to make the matrix and as time progresses, cells undergo keratinization and flatten to create the hard nail plate tissue. Closer to birth, the nail plate migrates over the nail bed tissue to reach the tip of the finger creating a "free edge." The eponychium tissue that once covered the nail disappears and results in the cuticle while the hyponychium is formed underneath the free edge of the nail.[17]

1.4 Nail Organ Traumatic Injuries

Various traumatic injuries are treated in both emergency rooms and primary care offices, amongst these injuries, damage to the nail organ is one of the most common. Nail organ injury is classified by the area of soft tissue damage and can be sustained by tearing the nail from its

surrounding tissue, resulting in lacerations and/or blood trapped underneath the fingernail. Closed or open nail injuries can be sustained by slamming a finger in a door or cutting the tip of the finger with an electric saw, 50% of these types of injuries will include a bone fracture. To increase the chances of restoring the original aesthetic appearance, primary treatment must include repair of the nail bed ridges (if applicable) and effective splinting. Chronic appearance of the nail plate can provide clues about the traumatic injury and further delineate the region primarily affected. To achieve successful healing of the nail organ tissue and decrease the risk of secondary deformities, providers should possess a thorough understanding of traumatic nail injuries and have an appreciation for the variability in injury severity.

1.4.1 Crush Injuries

Blunt trauma to the nail's soft tissue is often the result of incidents such as closing fingers in a door or compressing fingertips in heavy machinery. These type of injuries, identified as crush injuries, can be associated with subungual hematoma formation, or build-up of blood causing pressure underneath the nail plate. While these types of hematomas [18] can be small, larger and more severe hematomas (covering more than 50% of the nail bed and separating the nail plate from the nail bed) can be quite painful and result in an unfavorable appearance.[19]

1.4.2 Nail Avulsion

Traumatic nail avulsions occur when the nail plate is forcibly detached from the underlying nail bed. This type of injury may involve tearing of the nail plate from its position underneath the proximal nail fold, while concurrently resulting in injuries to the soft tissue such as lacerations or fractures. The degree of avulsion may drastically affect the nail matrix along with the nail bed. Thus, salvaging the original nail plate, including the soft tissue matrix if present, is ideal.

1.4.3 Nail Lacerations and Fingertip Amputations

Open injuries, such as lacerations and amputations, are a result of sharp objects penetrating the nail organ and/or the distal phalange. Physicians use Allen's classification to report the magnitude of the traumatic injury to the fingertip, which organizes injury type based on which soft tissues are affected (**Figure 3**).[20,21] Hirase developed his own classification system defining distal

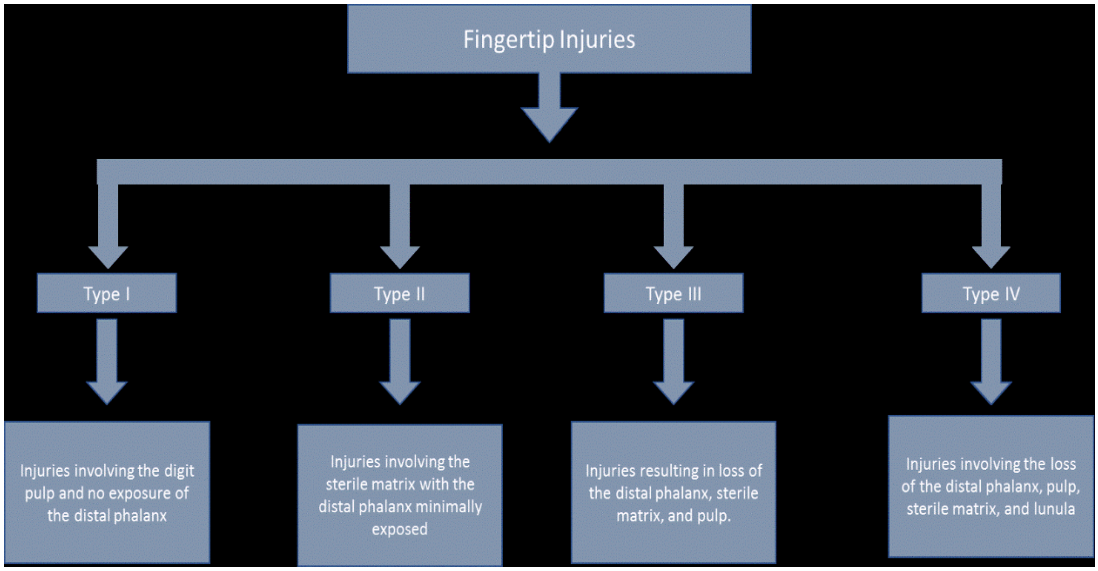

Figure 3. Allen's classification of fingertip injuries. Traumatic damage to the fingertip is classified based on the tissues affected (Type I-IV).[20,21] Illustration by Aundrya B. Montgomery.

phalanx (DP) amputations, giving clinicians a system to describe the zones of DP injury based on location.[21] These systems give clinicians an idea of possible treatment strategies needed for the case. Aesthetic outcomes of these injuries rely on its classification type and can range from ideal cosmetic outcomes to poor results such as hook nail or other unfavorable appearances of the nail.[22]

1.5 Clinical Treatment of Traumatic Nail Organ Injuries

A favorable prognosis following a traumatic nail injury is contingent upon the initial treatment strategy. Emergent treatment must be prompt and tailored to the type of soft tissue injury present. Treatments are established to address the specific injury type along with an important

consideration for the extent of injury severity. These strategies are tailored in numerous ways to decrease morbidity while concurrently preserving function and aesthetic appearance. While treatment methods may vary based on location and specialized expertise, all methods are conducted with the intent for complete regeneration.

Injuries affecting the nail bed, the distal portion of the matrix where the nail plate attaches, often requires surgical intervention. An intervention is required if there is a subungual hematoma that extends over 50% of the nail bed. The surgical repair involves removal of the nail plate to evaluate for the presence of soft tissue damage. Nail bed repair is necessary if tissue lacerations are present. Following repair, a nail splint is applied to inhibit fusion of the matrix to the proximal nail fold and eponychium.

The repair of nail injuries can occur under numerous conditions including local anesthesia, with a digital nerve block and tourniquet application, or in the operating room. Regardless of the repair strategy, one should always consider procedure time, post-operative recovery, and prognosis of phenotypical results. Crush injuries, nail avulsions, and nail lacerations with and without fractures may necessitate different treatment approaches that include split or full thickness grafts, v-y advancement flaps, or hematoma relief.[6] While treatments vary based on severity, a common practice is to splint the nail organ to facilitate a less painful, yet time conserved, healing process.

1.5.1 Nail Bed and Distal Phalanx Fracture Repair

Traumatic injury to the nail organ is often coupled with some type of damage to the nail bed's soft tissue, such as a subungual hematoma or laceration.[23] These types of injuries come with a high risk of uncertain prognosis when the initial treatment is either delayed or if the nail bed tissue is not meticulously repaired to promote smooth outward growth of the nail during the healing process.[24] Often, patients with acute traumatic injuries undergo a digital block under local

anesthesia so that the nail plate can be removed to debride and physically observe the extent of injury. If the nail bed is unharmed, the native nail, if available, or a prosthetic splint is placed in the proximal nail fold to promote outward nail growth as well as protect the nail bed during the healing process.[25] If lacerations are found, the physician will suture the wound being careful to avoid damage to other crucial regions for nail growth, such as the proximal nail matrix. Alternative suturing methods, such as the application of Dermabond to nail bed lacerations can be completed at a must faster rate than suture repair while maintaining similar functional and aesthetic prognoses.[24] If the distal phalanx is fractured due to a crush injury for example, the bone can be fixed using Kirschner wires and further stabilized using the nail for additional support.[26]

1.5.2 Grafts

The use of split- or full-thickness grafts are selected when there is significant tissue loss of the germinal matrix and/or nail bed tissue that primary repair of the nail organ's soft tissue is not feasible, this can be seen in some cases of laceration repair. Donor tissue is excised from germinal matrices and nail beds of adjacent fingers or the patient's toe and then sutured over the missing tissue to promote regeneration.[27] Clinical results have demonstrated that split-thickness nail bed grafts result in less nail deformities, promote nail adherence, and decrease donor site morbidity, while the use of full-thickness grafts consistently caused donor site morbidity in many cases.[28,29] For years, split-thickness grafts were preferred over to full-thickness grafts; however, disadvantages such as poor nail adherence to the graft prompted the need for a revised strategy, hence the introduction of thin split-thickness grafts. These translucent grafts, often taken from the toenail bed, were devised to decrease donor site morbidity commonly associated with full-thickness grafts.[30] Composite grafts, composed of sterile and germinal matrix tissue, have been used in nail deformity reconstruction in both adult and pediatric cases, but the prognosis is

unpredictable and could require secondary treatment for subsequent deformities.[31,32] Recently, single-layer bovine acellular dermal grafts have been applied in reconstructive procedures, but they are only applicable in repairing damage to the nail bed.[33]

1.5.3 Flaps

When replantation is not an option, flaps are used to reduce the shortening of the digit tip and to assist with elongation of the nail bed.[34] In efforts to retain the original phenotype of the nail bed, flaps are often coupled with nail bed grafts to assist with the regeneration process. Advancement flaps are used in cases where the distal phalanx is exposed, typically occurring in more proximal amputation cases, and the type of flap used is based on the geometry of the digit tip injury. For instance, Hwang's group suggests the use of V-Y advancement flaps in patients that have either dorsal oblique or transverse injuries, while those with volar oblique injuries were treated with abdominal flaps.[35] Cross finger fascial flaps can be used if the germinal matrix is present, but secondary treatment is needed to modify the flap and nail deformities are possible due to the tension of the suture applied to the nail bed graft.[36] Thenar fascial flaps, combined with nail bed grafts, were performed on nine patients and had successful outcomes, however, pitfalls such as low sample size, lack of graft vasculature, and an increased chance of flexion contracture require more attention to improve the surgical strategy.[37] Although multiple flap techniques have been established, many of them share the same disadvantages, further exemplifying a need for the development of a procedure capable of regenerating native-like digit tip tissues.

1.5.4 Replantation

Digit replantation procedures, first conducted by Komatsu and Tamai in 1967, have been used in efforts to restore the native function and appearance of the nail organ prior to traumatic injury.[38] Proper preservation of the amputated tissue remains a pillar for successful replantation.

Preoperative hot and cold ischemia must be managed and reducing the former while regulating the latter is necessary to appropriately salvage the amputated tissue.[39] Fingertip replantation procedures have great success when the amputation level is proximal to the nail organ, however, when the amputation is located more distally, treatment strategies vary due to challenges of a vein anastomosis.[21] According to Nishi et al., successful nail regeneration after amputation relies on three crucial factors, location of the amputation, vascular presence, and the extent of damage to both the nail matrix and nail bed.[40]

1.6 Importance of Nail Regeneration: Taking a Regenerative Engineering Approach

Many decades of research have been dedicated to the regeneration of complex tissues. Tissue engineering has focused on engineering biocompatible substrates efficient in accelerating the regeneration of damaged complex tissues.[41] Scientists have contributed to the field of tissue engineering to develop strategies to improve the quality of life of patients suffering from skeletal injuries. Tissue engineering applies biological, chemical, and engineering principles to regenerate tissues *in vivo* and *in vitro*. Over the years, there have been advancements in regeneration of specific tissues, however this interdisciplinary approach has faced limitations when translating to the clinical arena.[42] To overcome these limitations, a transdisciplinary approach was established, an emerging field of science referred to as "Regenerative Engineering." It is defined as the convergence of Advanced Materials Science, Stem Cell Science, Physical Forces, Developmental Biology, and Clinical Translation for the regeneration of complex tissues and organ systems. Regenerative engineering strives to combine established methods from each discipline to enhance regenerative outcomes.[43]

Regenerative engineering expands the principles of tissue engineering by utilizing recently established cell biology and practicing cutting-edge techniques, such as using induced pluripotent

stem cells and other adult stem cell populations, to regenerate target tissue types. The addition of developmental biology provides an avenue for understanding embryonic developmental and utilizing similar principles for the regeneration of tissue within the adult.[44] Understanding physical forces further elucidates how cellular processes such as movement alters cellular morphology, and how unknown forces can contribute to regeneration of native tissues.

Advanced material science has progressed towards improving biocompatibility and constructing biomaterials to mimic the extracellular native environment. Breakthroughs in advance material science have allowed bioengineers to tailor the properties and characteristics of biomaterials to better enhance the regeneration of tissues *in vitro* and *in vivo*.[42] Synthetic materials, preferred over natural materials, are used as delivery systems to aid in accelerating the regeneration process.[45] These materials are fabricated using various methods including 3D printing, self-assembly, and electrospinning.[46] Regeneration of damaged tissues relies upon replicating the correct structure of the extracellular matrix, activation and inhibition of regenerative related signaling pathways, and restoration of native tissue function. Advances in material sciences have made it possible to mimic these biological structures, therefore leading to improvements in regenerative medicine strategies.

Regenerating a human nail and digit is an ongoing goal within the field of Regenerative Engineering and harnessing the field's expertise puts scientists at an advantage in accomplishing this task. The complex anatomy of the human limb makes the task of regeneration complicated in the sense that a man-made engineered design must exactly mimic the blueprint of the native intrinsic design to ensure the correct function of the regenerated nail and digit. The grand challenges of molecular biology include inducing regenerative and competent signaling pathways without stimulating inhibitory or hyperactive signals. This is crucial for preventing processes that

can be detrimental to the regenerative process.[47] The biomaterial network, composed of a multitude of scaffolds with various designs, must not only mimic the proper extracellular environment, they must also possess the correct properties such as tailored degradation rate and other mechanical properties equivalent to the targeted tissue phenotype. Engineering a biomimetic system composed of biocompatible materials functionalized with stem cells and other biologically active molecules are essential in assisting the regeneration of a human nail and digit. Further elucidation is imperative to unmask human ability to regrow these complex tissues.

Human nail and digit tip regeneration includes the regrowth of multiple tissue types and moreover, requires the input from multiple fields of science. More broadly, whether regenerating a fully functional fingertip or morphologically correct fingernail, interdisciplinary approaches must be made to understand intrinsic details necessary for successful regenerative processes. The field of Regenerative Engineering has continued to make conscious efforts in regenerating complex tissues via areas of developmental biology, advance material sciences, stem cell research, physical forces, and clinical translation. Developing regenerative engineering strategies, including the fabrication of biomimetic extracellular scaffolds and isolation of proper stem cell populations, will be of significance whilst evaluating the nail organ's contribution to both mammalian nail and digit tip regeneration.

Benefits of developing a cost-effective and biocompatible method to repair both traumatic nail injuries and chronic nail deformities remains two-fold. Both mammalian nail and digit regeneration share some relation and understanding the phenomena by which the nail organ participates in the processes could possibly contribute to the regeneration of these complex tissues.[6,48-50] Understanding the anatomy of the nail organ will allow scientists to develop regenerative engineering techniques while addressing the disadvantages of nail damage commonly

treated in the clinic and operating room. Constructing a biodegradable, functionalized biomimetic matrix composed of an FDA cleared, inexpensive polymer will not only assist with the regeneration of hard nail tissue but could possibly be applied to future digit amputee cases.

Chapter 2: Isolation and Characterization of Nail Progenitor Cells Harvested From Nail Matrix Region

2.1 Introduction

Comparable to skin and its appendages, the nail organ houses its own "modified" epidermis.[51] The nail matrix, more specifically the sterile or proximal matrix, is responsible for the constant proliferation of stem cells that ultimately give rise to the hard nail plate. Nail stem cells (NSCs), found at the stratum basale of the nail's soft tissue, continuously proliferate and give rise to daughter cells that migrate up through the stratum spinosum and stratum granulosum layers. Differentiated NSCs, also called keratinocytes, reach the final stage of terminal differentiation at the stratum corneum where they are flattened and packed together forming the hard nail plate.[52] The outward growth of the nail is due to the continuous proliferation of NSCs unlike the cycles in which the hair follicles undergo growth. Thus far, the biology of NSCs still remain elusive in regard of their contribution to both nail organ regeneration and digit tip regeneration seen in mammals. Studies have shown that the presence of the nail matrix is crucial in the regenerating injured nail and/digit tip tissue and in reconstructive procedures, the nail bed should be repaired efficiently in order to restore favorable downstream aesthetic appearances.

2.2 Materials and Methods

2.2.1 Materials

Male Sprague-Dawley (6-8 weeks old) rats were purchased from Charles River Laboratories, (Wilmington, MA) All animal handling and procedures were carried out in accordance with the Institutional Animal Care and Use Committee at the University of Connecticut Health Center, Farmington, CT.

EpiLife media, minimum essential media, DMEM/F12-K, fetal bovine serum, and Penicillin/Streptomycin were all purchased from Thermo Fisher Scientific (Waltham, MA).

Insulin from bovine pancreas, epidermal growth factor (EGF), $CaCl_2$, and hydrocortisone were purchased from Sigma Aldrich (St. Louis, MO). Accutase was obtained from MilliporeSigma (Burlington, MA). Quant-iT™ PicoGreen™ dsDNA Assay, TRIzol reagent, *K15, K14, K31, Lgr6, Ivl*, *Anpep*, and *GAPDH* oligonucleotides (**Table 1**) were purchased from ThermoFisher Scientific (Waltham, MA). RNA to cDNA EcoDry™ Premix was purchased from Takara Bio, Inc. (Mountain View, CA). iTaq Universal Probe Supermix was obtained from Bio-Rad Laboratories (Hercules, CA). CD29 (1:100), CD90 (1:100), Lgr6 (1:50), K15(1:100), and K10 (1:100) primary antibodies and AlexaFluor® 488 and 594 secondary antibodies were purchased from Abcam (Cambridge, MA). CellTiter 96® AQ_{ueous} One Solution Cell Proliferation Assay (MTS) was purchased from Promega (Madison, WI).

2.2.2 Methods

2.2.2.1 Nail Stem Cell Isolation

Nail stem cells (NSCs) were isolated from the proximal nail matrix of 6-8 week old Sprague-Dawley rats. Briefly, separation of the hard nail plate and the proximal nail fold revealed the underlying matrix tissue for harvest. The distal matrix was disposed of and proximal nail matrix tissue was isolated for explant culture. Nail matrix samples were washed three times with PBS containing 1% P/S before culturing. Matrices (30 proximal nail matrices) were cultured in EpiLife media supplemented with 10% FBS, 1% P/S, and 0.06 mM $CaCl_2$ at 37 ^oC containing 5% CO_2. Media was changed every 2 to 3 days.

2.2.2.2 Effect of serum on NSC culture

NSCs were cultured with 0, 5, and 10% serum containing DMEM/F-12K medias (1% P/S) for 2 and 7 days. NSCs were lysed to harvest DNA and the Quant-iT™ PicoGreen™ dsDNA Assay was used to measure the DNA content within the samples. Excitation was measured at 480 nm.

2.2.2.3 Flow Cytometry

NSCs were removed from tissue culture flasks via accutase and suspended in PBS containing 3% FBS. Cells were separated into Eppendorf tubes at $1.0x10^5$ densities and K10, CD29, CD90, K15, and Lrg6 primary antibodies were added and incubated for 1 hour at 4°C. Cells were centrifuged at 4 g for 5 minutes and the pellet was washed with PBS/3% FBS solutions three times. Cells were then fixed with 4% paraformaldehyde for 20 minutes, centrifuged, and washed with PBS 3 times. Secondary antibodies (AlexaFluor® 488 and 594) were added to samples and incubated for an additional hour. NSCs were then centrifuged and washed 3 times, then taken for flow cytometry analysis.

2.2.2.4 Calcium Dependent Differentiation Studies

NSCs were seeded at $2.5x10^5$ per well and washed with PBS prior to treatment. Cells were subject to treatment with EpiLife media containing 0 mM (0) or 0.06 mM (low) $CaCl_2$ media or high calcium media containing 1.87 mM $CaCl_2$, methods similar to those reported by Nagae et al. and were cultured for 3, 7, and 14 days. Media was changed every 2 to 3 days.[53]

2.2.2.5 RNA Extraction and qPCR Analysis

Cells were harvested at 3, 7, 14 days after treating with 0, low, and high $CaCl_2$ medias and washed with PBS before adding Trizol reagent and RNA was isolated based on the manufacture's protocol. RNA concentration was measured using the NanoDrop and was reversed transcribed using RNA to cDNA EcoDry™ Premix. Gene expression of *K15*, *Anpep*, and *Ivl* was detected using iTaq Universal Probe Supermix and oligonucleotide primers specific to the above stated proteins and normalized to the expression of GAPDH. ΔCT values were used to evaluate relative expression within the samples.

2.2.2.6 Metabolic effect of EGF on NSC culture

$3.5x10^4$ NSCs were cultured in 48-well plates containing DMEM/F12-K media supplemented with 0 ng/mL, 10 ng/mL, 50 ng/mL, or 100 ng/mL of EGF. Culture conditions were administered under serum and serum-free conditions at 3, 7, and 14 days. At endpoint, samples were incubated for 4 hours with MTS reagent and absorbance was read at 490 nm to measure NSCs metabolic activity.

Table 1. Oligonucleotide sequences of nail matrix related genes observed in PCR.

Gene	Oligonucleotide Sequence	Amplicon Length (bp)	Assay Location
Krt31	5' ACAAGCAACGCGTGCGGCAAGCCCATTGGGCCCTGCGTCTCCAATCCCTGCGCCCCCTGCCCACCCCCTG CCCCTTGCACACCTTGTGTCCCACGTTCCCGCTGTGGGCCATGCAATAGCTTTGTACGCTAG 3'	71	1185
Krt14	5' AGCAGGAGATCGCCACCTACCGCCGTCTGCTGGAGGGCGAGGATGCTCACCTTTCATCTGCCCAATTCTC CTCATCGTCTCAATTCTCCTCTGGCTCTCAATCATCCAGAGATGTGACCTCCACCAACCGCCAGATCCGC ACCAAGGTCATGGATGTGCACGATGGCAAGGTGGTCTCCACCCACGAGCAGGTCCTGCGCACCAAGAACT AA 3'	114	1361
Anpep	5' TCACTCTGCCGCTGAGCAACACCCTCTTCCTGGCCAGTGAAACAGAATACATGCCCTGGGAGGCTGCCCT GAGCAGCCTGAACTACTTCAAGCTCATGTTTGACCGCTCGGAGGTCTACGGCCCCATGAAGCGCTATCTG AAGAAGCAAGTCACACCCCTCTTCGCCTACTTCAAAATCAAAACCAACAACTGGCTCGACCGTCCTCCAA CACTGATGGAGCAGTACAACGAAATTAATGCCATCAGCACCGCCTGTTCTA 3'	130	2173
Ivl	5' AAAGAAAGAAGCACAAATTGGAGAACCTGACACAGAAGGAGAAGCAGATAAAGCAATTAGTACCAAGCAC TGACAGAGTCCAAGAGACTCAGCCAATCCAACCAGTGAAAGAAGACTCTCTCACTACAAAGAAGCAGCAG CACAGCCATGAAGTGCAGTGA 3'	87	1634
Krt15	5' TCAGCACTTACCGGAACCTGCTTGAGGGCCAGGATGCTAAGATGGCTGCTATTGGTGTCAGGGAAGCATC CCTGAGAGGAGGCAGCAGCGGCGGTGGCAGCAATTTCCACATCAGCGTGGA 3'	60	1306
Krt10	5' GCCTGGAGAACGAGATCCAAACCTACCGCAGCCTGCTAGAAGGAGAAGGAGGGTATGTTGGAAACCTGCA AATAACCCTCAATTGCTTTCCTTCAGAATTCCACTTAGCAAAGCTTACCCAAACCCAAGGAAAAACCAGA GGCTGGAAGGGGAGCAATACTAATAAAACCAGAGTGATCAAGACGATTATTGAGGAGGTGACACCTGAGG GTAGAGTCCTTTCGTCTATGATTGAATCAGAAACCAAGAAACACTTCTACTAA 3'	145	1464
Lgr6	5' GGACAAGCTGAGAACCACTATGACCTAGACCTGGATGAGCTCCAGATGGAGACAGAGGACTCAAAGCCAC ACCCCAGTGTCCAGTGCAGCCCTGTTCCAGGCCCCTTCAAGCCCTGCGAGCACCTCTTTGAGAGCTGGGG CATCCGCCTTGCTGTGTGGGCCATCGTGCTGCTCTCGGTACTCTGTAACGGGCTGGTGCTG 3'	100	1870
GAPDH	5' AATGACAACTTTGTGAAGCTCATTTCCTGGTATGACAATGAATATGGCTACAGCAACAGGGTGGTGGACC TCATGGCCTACATGGCCTCCAAGGAGTAAGAAACCCTGGACCACCCAGCCCAGCAAGGATACTGAGAGCA AGAGAGAGGCCCTCAGTTGCTGAGGAGTCCCCATCCCAACTCAGCCCCCAACACTGAGCATCTCCCTCAC AATTCCATCCCAGACCCCATAACAACAGGAGGGGCCTGGGGAGCCCTCCCTTCTCTCGAATACCATCAAT AAAGTTCGCTGCACCCTCAAAAAAAAAAAAAAAAAAAAAAAAAAAAA 3'	174	1153

2.2.2.7 Statistical Analysis

Statistical analysis presented the mean ±SD of values calculated using one-way ANOVA analysis. p values that defined significance between samples, $p<0.01$*, $p<0.001$**, $p<0.0.0001$***, $p<0.00001$****

2.3 Results

2.3.1 NSCs Express Nail Matrix Related Cell Surface Markers

The nail matrix, located at the base of the insertion point of the hard nail plate into the nail fold, is dense with cells and can be viewed via hematoxylin and eosin staining **(Figure 4A-B**). Explant culture of primary NSCs from the nail matrix region of 6-8 week old male Sprague-Dawley rats displayed a cobblestone configuration around the periphery of the matrix tissue visible at 3 days in culture, similar to that observed in human nail stem cells in culture (**Figure 4C**).[54,55] Effects of serum conditions on NSC proliferation showed a significant decrease between 0% and 5-10% by day 7 in culture, suggesting that the NSC population could not sustain healthy growth and proliferation in a serum-free environment. Since there was no noticeable change between the 5% and 10% and to maximize the preservation of the NSC population, we decided to proceed with 10% serum conditions (**Figure 5**).

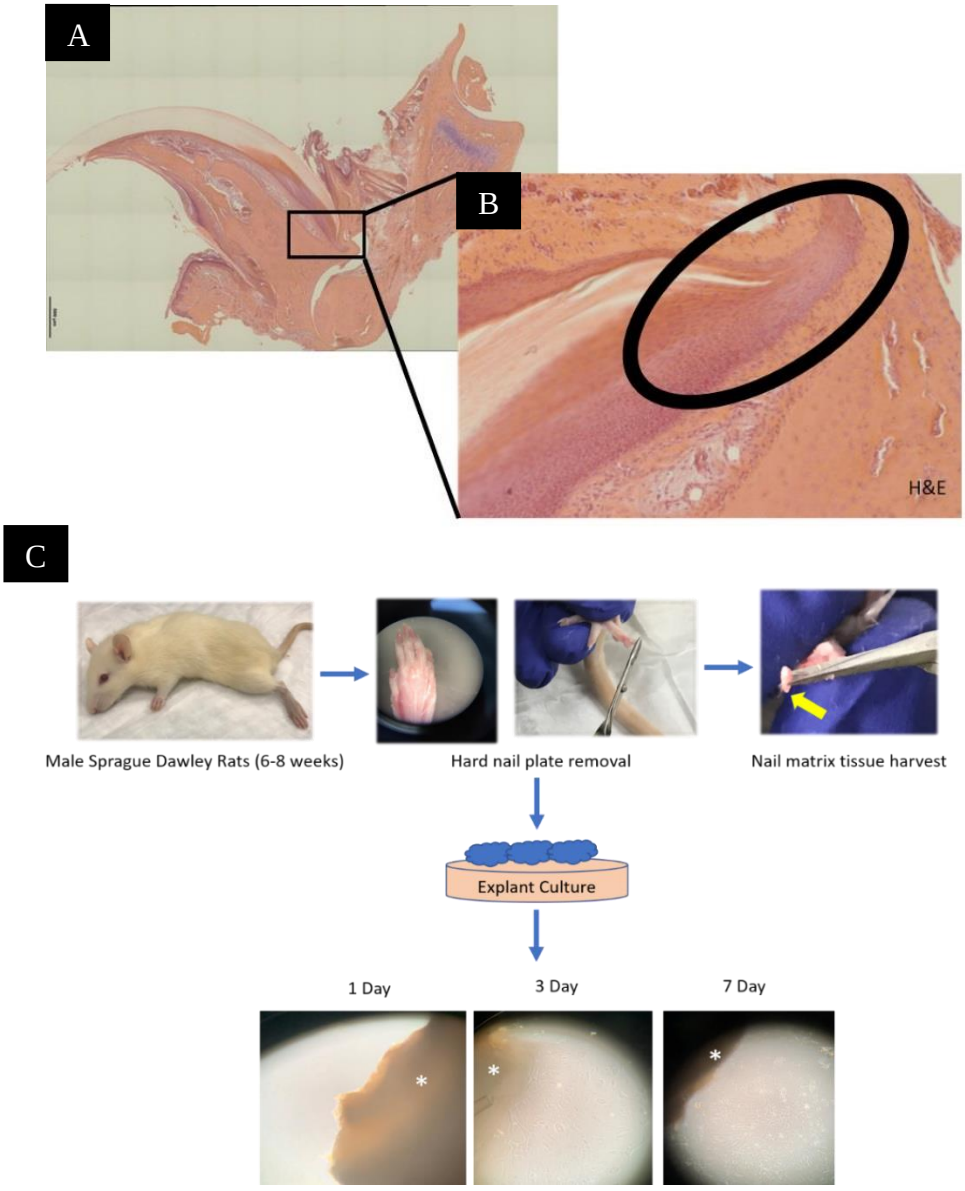

Figure 4. Isolation and Explant Culture of NSCs. **A.** H&E staining of 6-8 week old Sprague-Dawley rat digit. **B.** Zoomed in image of the nail matrix region that houses NSCs. **C**. Nail matrix tissue is harvested from the rat nail matrix and cultured via explant methods. Cells migrate out of explant tissue at three days and show confluent colonies at 7 days in culture before passaging. Asterisk denotes nail matrix tissue.

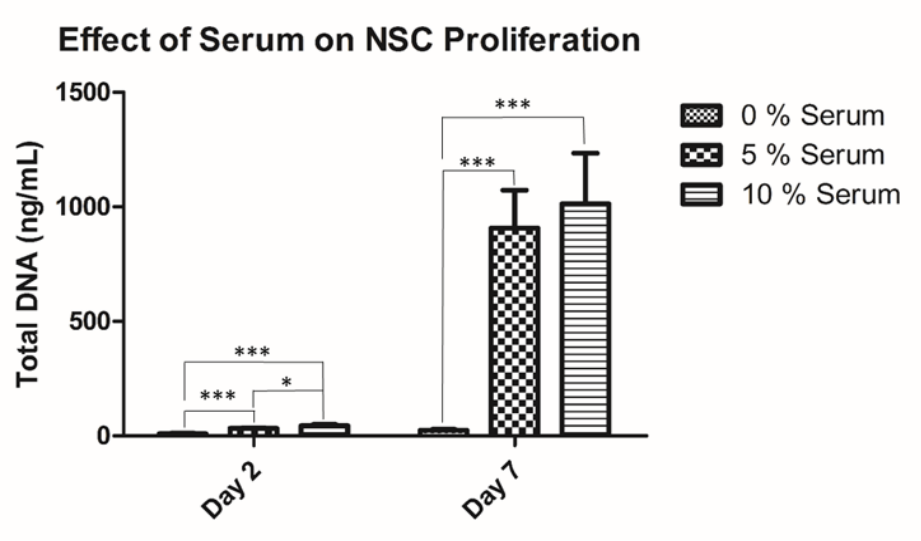

Figure 5. NSC proliferation based on serum conditions. P2 NSC DNA content was measured at 2 and 7 days after culturing in 0, 5, and 10% serum conditioned DMEM. Quant-iT™ PicoGreen™ dsDNA Assay showed a significant difference between 0% serum and 5-10% serum conditioned groups. No significance was noted between 5% and 10% serum groups at 7 days.

Passage 2 (P2) NSCs expressed Lgr6 (90.9%) , which has been found to mark NSCs, and CD90 (99.5%) and CD29 (99.4%), markers for epidermal stem cells (**Figure 6A-D**).[48,56-58] Flow analysis of double stained Lgr6/K10 NSCs shows limited expression (1.3%) of the K10, a suprabasal cornified epidermis marker (**Figure 7**).[56] As cells reached P3, Lgr6 expression was shown to decrease (immunocytochemistry data not shown), however, the presence of the epidermal stem cell marker, K15, is present and the presence of K10 is noted as well, suggesting that NSCs begin to undergo differentiation at this passage (**Figure 8A-B**). This can also be attributed to the confluency of the cell culture. At P4, the expression of both Lgr6 (7.7%) and K15 (4.8%) show a dramatic decrease, while the expression of K10 (30.6%) is increased (**Figure 9A-C**).

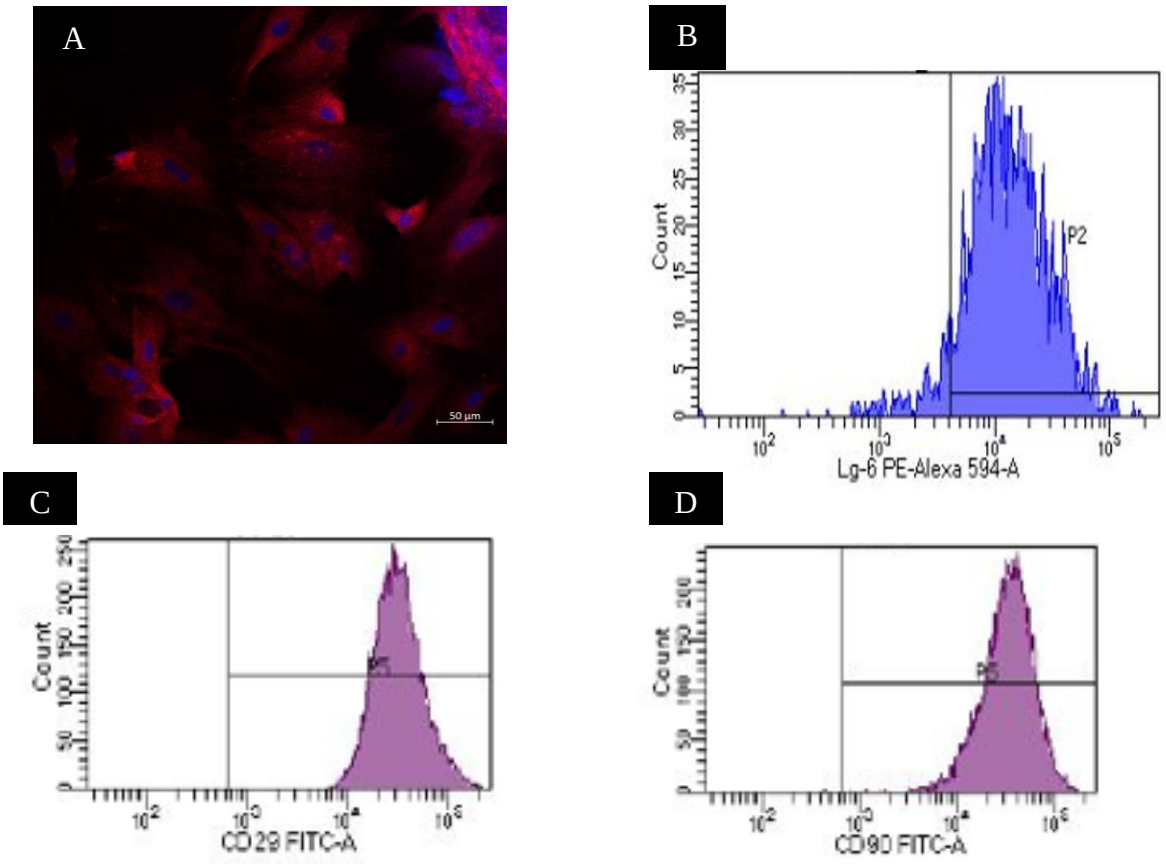

Figure 6. NSC expressing stem cell associated markers. **A**. Immunocytochemistry analysis of Lgr6 expression in P2 NSCs. (red) Lgr6 (blue) DAPI. **B-C**. Flow cytometry analysis of stem cell marker expression. **B**. Lgr6. **C**. CD29 and **D**. CD90.

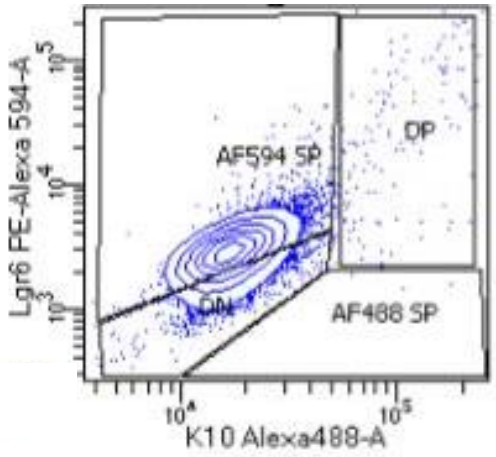

Figure 7. Expression of NSC marker Lgr6 in P2 NSCs. Flow cytometry analysis of double stained P2 NSCs with Lgr6 and K10 markers.

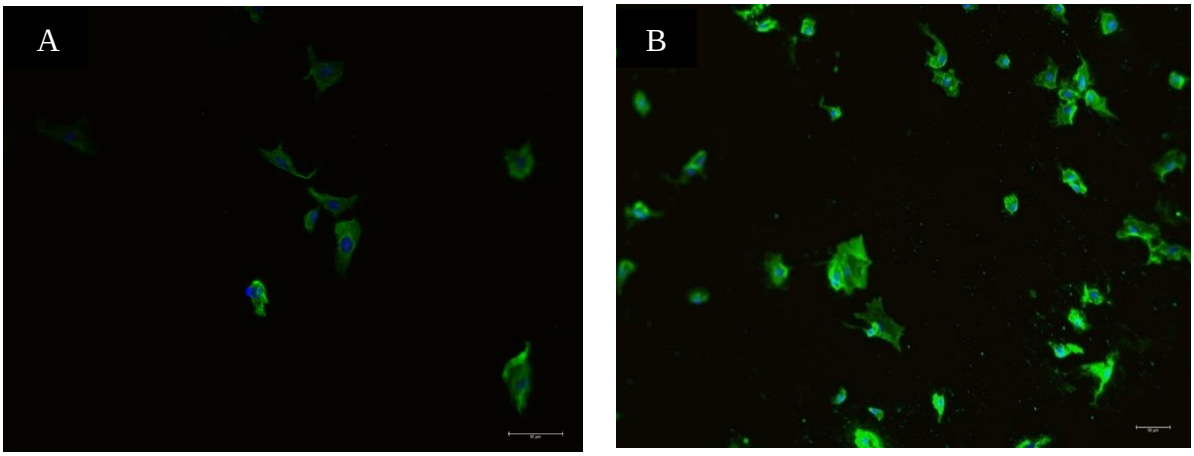

Figure 8. Immunocytochemistry of P3 NSCs. **A**. NSCs expressing epidermal stem cell marker K15 (green) DAPI (blue). **B**. Expression of K10 (green) and DAPI (blue) in P3 NSCs.

2.3.2 Calcium dependent gene analysis of NSCs

It is hypothesized that cells isolated from the proximal nail region can be differentiated into hard acidic keratins based on calcium concentration manipulation.[59] To confirm the presence of keratin and nail matrix related genes, we first tested oligonucleotide sequences for K15, K14, Anpep (also referred to as CD13, a marker associated with onchyofibroblasts specifically in the nail matrix)[60], and involucrin (a keratinocyte early terminal differentiation marker)[61] in the isolated nail matrix tissue and in NSCs exposed to 0 (0 mM), low (0.15 mM), and high (1.87 mM) $CaCl_2$ supplemented medias. K15, K14, and Anpep were expressed in the nail matrix tissue, but the presence of involucrin was not noticed (**Figure 10A-B**). The absence of this marker could either be due to the tissue sample not containing terminal differentiating cells, or the expression of the protein was at minimum levels in the tissue. K15, K14, and Ivl expression was not detected in the NSC culture, however, Anpep expression showed an ascending trend in conjunction with $CaCl_2$ levels. The same trend is noticed over 14 days of NSCs cultured with 0, low, and high $CaCl_2$ media

(**Figure 10C**). Taken the results of this study, we suggest that the primers for the identified genes are efficient, as seen in the matrix tissue, however, in cell culture conditions, absence of K15 and K14 could be due to a heterogeneous cell population within the sample outcompeting the NSCs in culture, therefore masking the expression of these stem cell genes. Although keratin stem cell markers were not observed in culture, *Anpep* expression is interestingly expressed throughout the 14 day cell culture.

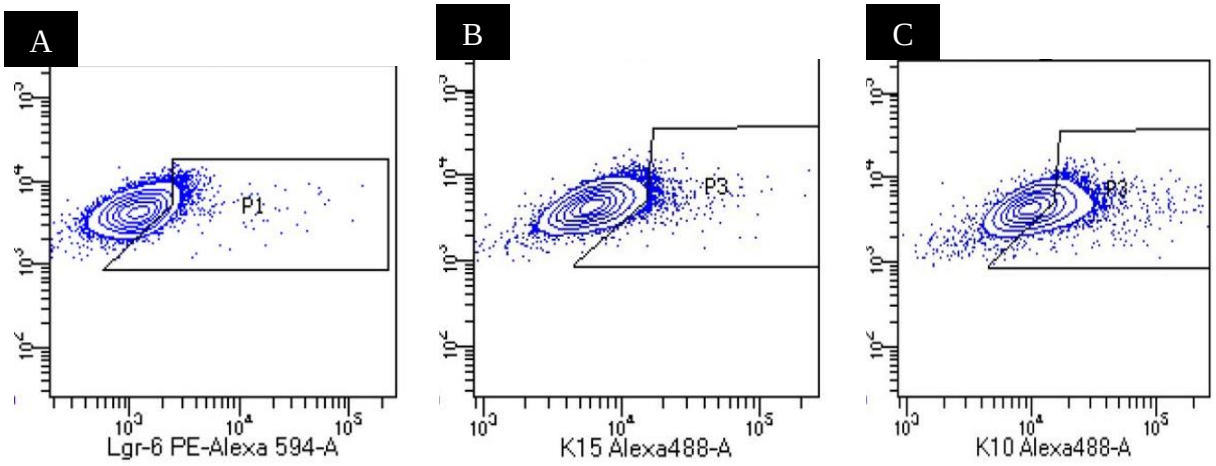

Figure 9. Flow Analysis of P4 NSC differentiation. A. Lgr6 and **B.** K15 show decrease in expression at P4. **C.** K10, differentiation marker, shows an increase in expression.

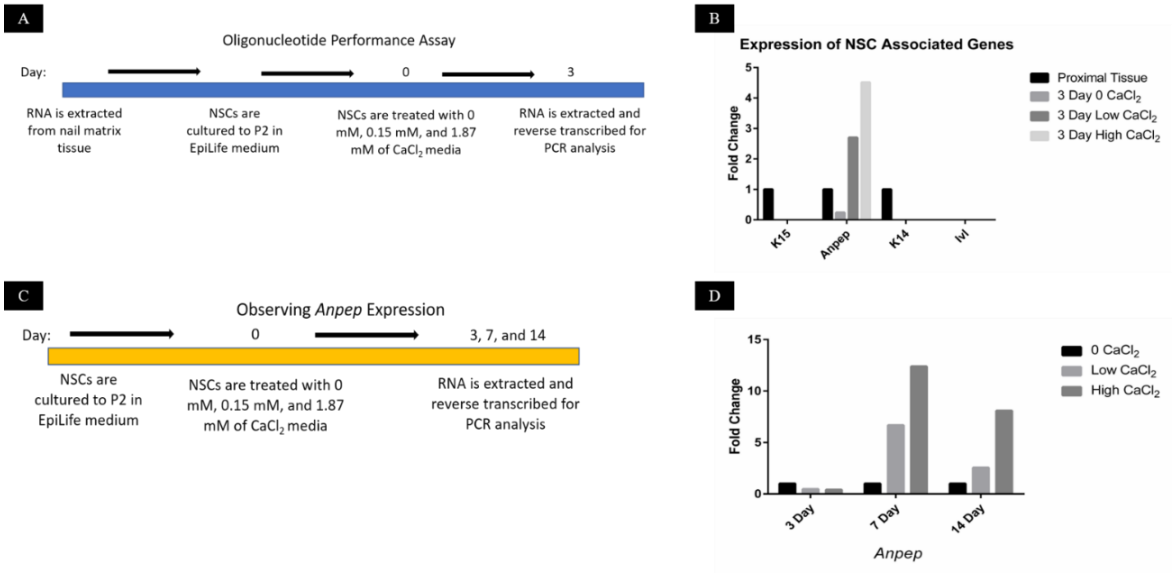

Figure 10. Evaluating the expression of nail matrix related genes. **A**. RNA was isolated from nail matrix tissue and P2 NSCs cultured in $CaCl_2$ supplemented media at 0, low, and high levels for three days. **B**. Expression of K15 and K14 are observed in nail matrix tissue, but Ivl expression is not noted in primary tissue samples or NSC culture. Anpep is expressed in proximal matrix tissue and in 3 day NSC cultures. **C**. NSCs treated with 0, low, and high $CaCl_2$ medias for 3, 7, and 14 days were subject to RNA isolation and reverse transcribed for PCR analysis of Anpep expression. **D**. Anpep expression is present in 3, 7, and 14 day NSC cell cultures and show ascending trend coupled with $CaCl_2$ media concentrations.

2.3.3 Determining NSC Proliferation as a Result of Epidermal Growth Factor

To observe NSC metabolic activity as a result of EGF treatment, cells were cultured in conditioned media containing 0 ng/mL, 10 ng/mL, 50 ng/mL, and 100 ng/mL of EGF for 3, 7, and 14 days (**Figure 11A**). In the presence of serum, NSC cultures remained viable at 14 days with the most noticeable increase observed at 7 days when cultured with 10 ng/mL of EGF (**Figure 11B**). However, when cultured in serum-free conditions, NSCs showed a significant decrease in metabolic activity despite the added concentration of EGF (**Figure 11C**). By 14 days, NSC cultures did not retain high viability as shown in the serum counterparts, giving the assumption

that EGF alone is unable to sustain NSC proliferation. This further solidifies our findings that NSCs require the addition of serum to maintain viable cultures.

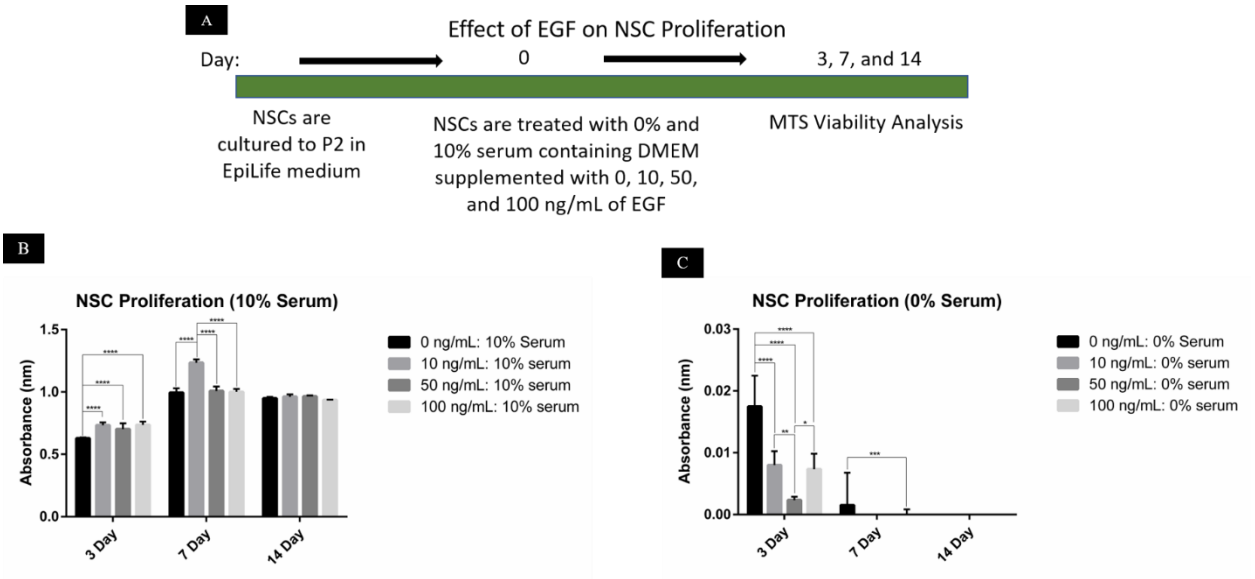

Figure 11. Effect of EGF on NSC proliferation. A. P2 NSCs were cultured for 3, 7, and 14 days in 0% and 10% serum containing EpiLife media supplemented with EGF at 0, 10, 50, and 100 ng/mL. MTS assay was used to evaluate NSC viability. **B**. 3 Day NSC cultures showed significance ($p<0.0001$) between groups treated with 0 ng/mL EGF and 10, 50, and 100 ng/mL treated groups. 7 day cultures revealed a significance increase ($p<0.0001$) between NSCs treated with 0 ng/mL and 10 ng/mL and a significant decrease between 50 ng/mL and 100 ng/mL samples when compared to the group treated with 10 ng/mL of EGF. No significance was noted between groups at 14 days. **C**. There was a noticeable decrease of NSC viability between 10 ng/mL, 50 ng/mL, and 100 ng/mL EGF treated groups compared to 0 ng/mL samples when NSCs were treated with 0% serum conditioned media. At 7 days, NSC viability continues to decrease in treated groups and by 14 days in culture, the NSCs viability is no longer detectable.

2.4 Discussion and Future Directions

The nail matrix has been found to be the source from which the hard nail plate extends from and if injured, along with the nail bed tissue, can affect down-stream functioning and aesthetic appearance of the nail organ. Clinical methods addressing traumatic nail injuries, more specifically to improve prognosis factors, require an adoptable strategy that can be used consistently over the broad spectra of trauma types and severities, easily accessible supplies for repair procedures, and initial treatment methods that can be quickly performed without compromising long term healing factors. Converging stem cell science and advance materials science to define strategies geared toward improving nail injury repair methods give way for us to mimic the nail's extracellular matrix using biomimetic substrates and functionalize the matrix with the addition of the stem cells responsible for creating the native tissue. Current materials used for nail splints lack bioactivity, thus giving hints at one of the causes contributing to unfavorable regenerative outcomes of the nail plate post repair.

In vitro culture conditions for NSCs have been defined previously in the literature and while monitoring our explant culture over time, we have observed many similarities to those reported by Nagae et al. and Picardo et al.'s analysis of this cell type.[53,62] NSC isolation posed challenges similar to that reported in Nagae et al.'s study such as small tissue sample size and inability of NSCs to grow in serum-free conditions as we were able to confirm as well.[53] To acquire enough cells to perform *in vitro* experiments, a minimum of n=3 rats (9 isolated matrices from the 2^{nd}-4^{th} hindlimb digits) were used in our explant cultures. We used digits from the hindlimbs to keep consistency within the samples due to the difference in growth rates between fingernails and toenails and also due to the small size of the front limb digits.[63] After 3 days in culture, we began to see cells migrate out of the nail matrix tissue (see Figure 4) and the NSCs

continued to follow the same growth trend previously reported.[53] We also visualized the morphology of explant cultured NSCs and found that the cell morphology exhibited a "cobble stone" appearance and morphological similarities to nail matrical keratinocytes and nail fibroblasts reported by Okamoto et al.[53,55]

Due to the small tissue size, we were unable to achieve enough NSCs for further experiences until P2-3. Once cultures yielded ideal cell number, further characterization to determine if factors such as proliferation and differentiation could be manipulated to stimulate the production of keratinized tissue. Initial characterization revealed that cultured NSCs expressed Lgr6, K15, CD90, CD29 stem cell markers, consistent with previous findings and suggesting that our culturing technique and conditions are able to sustain NSC expansion.[48,54] Gene expression analysis of NSCs remain elusive and understanding biological cues that are present during homeostasis and upon differentiation could prove useful when defining techniques to apply to nail tissue regeneration.

The nail plate is composed of stratified hard-keratinized epithelia, type I acidic keratins, produced by the suprabasal keratinocytes found in the nail matrix.[64] Previous findings have reported that *in vitro* levels of calcium increase the expression of hard keratins at high calcium concentrations.[62] Type I keratins K15 and K14 were expressed in the isolated proximal matrix tissue and interestingly, *Anpep* was present in both our tissue samples and NSCs treated with calcium medias up to 14 days in culture. We also evaluated the presence of Lgr6 and K31, markers specific to the nail matrix, and terminal differentiation markers, Ivl and K10 (data not shown) and were unable to detect expression levels. The nail matrix is not a defined anatomical structure, thereby resulting in a heterogenous population that could possibly exist in our cell cultures. Furthermore, taking into consideration the morphology of our explant cell population that

resembled both nail matrical cells and nail fibroblasts reported by Nagae et al. could suggest that the cobblestone cells, or NSCs, that we visualized at the initial stages of the explant culture could be outcompeted by the nail fibroblasts, also termed onychofibroblasts as denoted by the consistent expression of *Anpep*. Interestingly, the similar trend in expression of *Anpep* across the time points of samples suggest that it is calcium responsive which supports previous findings that attribute the role of CD13 in transducing intracellular influx of calcium.[65] The absence of K10 and Ivl in the nail matrix tissue is expected due to the tissue being the source of NSCs, however, we would expect to see the presence of these genes in NSC cultures, especially those introduced to high calcium at longer time periods. NSCs were cultured in standard DMEM:F12k media supplemented with 10% serum for 6 weeks (data not shown) and a hard matrix was found deposited in the culture dish. Raman spectroscopy results were insufficient in determining the matrix components to due peak overlap with the polystyrene material of the tissue culture plate and were unable to be repeated due to the NSCs low attachment to glass bottom dishes, which is the substrate needed for appropriate Raman analysis. This shows that our NSC population has the potential to produce matrix, but further optimization of *in vitro* conditions to stimulate this process. Combining these findings with our gene expression results give the suggestion that our culture conditions are unable to support the differentiation of the NSCs and future studies should include further optimization geared toward stimulating the expression of terminal differentiating genes in NSCs.

When considering treatment methods for traumatic nail cases, one must consider the process of wound healing and growth factors secreted in response to injury. EGF has been found to play a role in the recruitment of fibroblasts and other cell types to the region of injury during wound healing and promote other downstream mechanisms important for proliferation and de-differentiation of keratinocytes to assist with wound closing.[66] Currently, EGF is one of the most

widely used growth factor in clinical applications and is often used as a topical agent or given via injection to assist with the wound healing process.[67] In tissue engineering applications, EGF has been found to induce the expression of K14 *in vivo* and promote wound healing and re-epithelization of injured tissues.[68] In the present study, we attempted to rule out the masking of serum in regard of EGF response, however, serum-free conditions are unable to support NSC proliferation after 7 days. Future studies should include other *in vitro* techniques such as scratch assays to evaluate NSC response to EGF in terms of cell migration.

Understanding NSC physiological fundamentals has significant value when devising strategies to regenerate the hard nail plate, however, in the clinical setting, the use of NSCs is not feasible. Autologous grafts are currently used, but are not favored due to the risk of donor site morbidity. An easily obtainable and expandable cell population is necessary in order to create a scalable treatment technique for the clinic and to avoid risks such as immune rejection, an autologous cell source would be ideal. Future studies could evaluate reprogramming a widely available cell source such as adipose-derived stem cells into epidermal like cells could possibly serve as a autologous graft source to functionalize bioengineered nail splints.[69,70]

Chapter 3: Evaluating Nail Stem Cell Behavior on Biomimetic Electrospun Matrix *In Vitro*

3.1 Introduction

The hard nail plate not only assists with mechanical movement, but also functions as a protective barrier to the nail's soft tissue beneath. Upon traumatic injury, this protective shield is compromised and although the nail plate can be conserved and used as a natural splint during healing stages, this is not always the case. When devising strategies to engineer a readily available nail splint, factors such as biocompatibility, cost, FDA-clearance, and practical use of the system must be considered. Poly(lactide-co-glycolide) (PLGA), a widely preferred synthetic polymer that is known for its biocompatibility, tailorable degradation rates, and use in many scaffolding techniques. This material has been widely studied in our lab, and its potential to support cell proliferation and migration.[71] PLGA also has valuable physical properties such as mechanical strength. The fingernail is made of hard keratinized tissue that protects the fingertip and also assists with other mechanical movements that can be affected if the nail organ is not functioning as it was before injury took place. The nail plate does a phenomenal job of protecting the soft tissue of the nail bed and matrix, but upon traumatic injury, severe pain can occur if secondary injuries make contact or the freshly repaired tissue is not splinted correctly. It is important that the nail splint is sturdy enough to protect the delicate matrix and nail bed, but also has porous hydrophilic properties to attract cell proliferation and to be able to soak up drainage from the wound site to decrease on infections that occur as a result of fingertip repair. Gelatin, a hydrolyzed form of collagen, has been shown to promote cell adhesion, migration, and proliferation due the presence of the RGD peptide.[72] Gelatin can provide the hydrophilic nature to the scaffold which we need to assist with cell attachment, migration, and proliferation.

On a microscopic level, however, it is important to construct biomimetic matrices, or substrates that resemble the native extracellular matrix in specific tissues found in the body. Stem

cells, more specifically the ones found in the nail matrix, are constantly proliferating and differentiating into hard cornified tissue to maintain homeostasis of the nail organ. The nail matrix's ECM resembles a fibrous structure and mimicking this environment could assist with downstream efforts of transforming basal layer NSCs to hard-cornified epithelia in the stratum corneum. To combine physical properties of both PLGA and gelatin, coaxial electrospinning was chosen to fabricate a biocompatible fibrous scaffold for *in vitro* analysis to observe its potential to function as a bioactive nail splint for *in vivo* analyses of traumatic nail injuries.

3.2 Materials and Methods

3.2.1 Materials

Poly(lactide-*co*-glycolide) (PLGA) 85:15 was purchased from Lactel Absorbable Polymers (Birmingham, AL). Gelatin (Type A) was obtained from MD Biomedicals, LLC (Solon, OH). 1,1,1,3,3,3-Hexafluoro-2-propanol (HFIP), collagen I solution, methanol, and 4% paraformaldehyde solution were purchased from Sigma-Aldrich (St. Louis, MO). Glutaraldehyde (GA), Alamar Blue Assay, Crystal Violet, Rhodamine Phalloidin stain, EpiLife media, minimum essential media, fetal bovine serum, Penicillin Streptomycin and Gelatin from Pig Skin Fluorescein Conjugate (FITC-gelatin), and Hexamethyldisilazane (HMDS) were purchased from ThermoFisher Scientific (Waltham, MA). Accutase was obtained from MilliporeSigma (Burlington, MA).

Male Sprague-Dawley rats (6-8 weeks old) were purchased from Charles River Laboratories, (Wilmington, MA). All animal handling and procedures were carried out in accordance with the Institutional Animal Care and Use Committee at the University of Connecticut Health Center, Farmington, CT.

3.2.2 Methods

3.2.2.1 Coaxial Electrospinning

PLGA (shell) 10% w/v and gelatin (core) 4% w/v and 11% w/v gelatin (shell) and 11% w/v PLGA (core) (From this point further denoted as $Hybrid_1$ and $Hybrid_2$, respectively) solutions were used to fabricate nanofibers. Briefly, PLGA and gelatin were dissolved overnight in HFIP to use for the coaxial electrospinning method. For $Hybrid_1$ fibers, the needle-to-tip distance was 22 cm, applied voltage was 16 kV, and flow rate for the shell fibers was set at 1.0 mL/hour and core fibers at 0.5 mL/hr. $Hybrid_2$ fibers had a needle-to-collector distance was 30 cm, 22 kV was applied, and the flow rate for shell fibers was 1.30 mL/hr and core fibers was 0.850 mL/hr. Fiber mats were collected on aluminum foil (0.3±0.1 mm thick) then placed under vacuum for 48 hours to rid scaffolds of residual solvent.

3.2.2.2 Glutaraldehyde Vapor Crosslinking

Based on modified methods similar to Nguyen and Lee, $Hybrid_2$ scaffolds were exposed to glutaraldehyde (GA) vapors 25% v/v for 1 hr at 37^{o}C to complete the crosslinking process.[73] Scaffolds were then placed under vacuum for 48 hours to rid scaffolds of residual GA.

3.2.2.3 Physical and Chemical Characterization of Hybrid Fibers

Morphology of hybrid scaffolds was observed using scanning electron microscopy (SEM). Samples were sputter coated with Polaron E5100 then taken for imaging using the FEI Nova NanoSEM 450. Transmission electron microscopy (TEM) was used to confirm the encapsulation of core-fibers during the coaxial electrospinning process. To further confirm successful coaxial electrospinning parameters, PLGA and $gelatin^{FITC}$ containing solutions were electrospun using the previously stated parameters to yield $Hybrid_{1\_FITC}$ and $Hybrid_{2\_FITC}$ fluorescent fiber mats. The

scaffolds were imaged using confocal microscopy to observe the intensity of FITC within the samples.

3.2.2.4 Swelling Study

To analyze the hydrophilicity characteristics of hybrid scaffolds, 0.3±0.1 mm thick scaffolds ($Hybrid_1$, $Hybrid_{2\_UCL}$ and $Hybrid_{2\_CL}$) were cut into 1.5 cm x 1.5 cm squares and the dry weight was measured. Samples were then submerged in PBS and incubated at 37ºC for 1, 3, 7 days. At each time point of interest, scaffolds were harvest and wet-weight was measured. Samples were dried and taken for SEM analysis.

$$\%\ percent\ swelling = \frac{(wet\ weight - dry\ weight)}{dry\ weight}\ x\ 100$$

3.2.2.5 NSC Attachment

Briefly, scaffolds were cut in 1.5 cm x 1.5 cm squares then subjected to UV sterilization for 30 minutes per side. Scaffolds were then incubated in EpiLife media solutions containing 10% FBS and 5% pen/strep for 24 hours. $1.0x10^5$ cells were seeded $Hybrid_1$ and $Hybrid_2$ scaffolds then fixed with 4% paraformaldehyde solutions at 0 min, 30 min, 1 hour, 8 hours, and 24 hours. Hybrid scaffolds without cells were used as control. After the final timepoint, samples (n=4) were stained with rhodamine phalloidin and taken for confocal imaging. Samples were incubated with crystal violet reagent for 5 minutes then rinsed with PBS until the solution remained clear. 100% methanol was then added to dissolve the samples and the absorbance was read at 590 nm.

3.2.2.6 SEM to observe NSC attachment

NSCs (seeding density of $1.0x10^5$ cells) were seeded on Hybrid scaffolds and cultured for 24 hours. At each time point, samples were submerged in 1% GA solution for 1 hour at room temperature then fixed for 24 hours in 3% GA solution at 4 ºC. Scaffolds were subjected to serial

dehydration (30% 50%, 70%, 90%, and 100% ethanol) then incubated with various Hexamethyldisilazane (HDMS)/Ethanol solutions. Samples were allowed to air dry and desiccated until ready for SEM imaging.

3.2.2.7 Hybrid scaffold protein surface modification

$Hybrid_1$ and $Hybrid_2$ mats were cut into 1 cm x 1 cm squares and underwent UV sterilization for 1 hour (30 minutes per side). Using methods similar to those reported by Mansour et al., fibers were then soaked in collagen I solutions for 5 hours at 4^oC and then washed three times with PBS to removed excess collagen solution. Fibers were then soaked for 12 hours in PBS solutions containing 15% FBS and 5% P/S prior to seeding NSCs.

3.2.2.8 Alamar Blue Viability Studies

NSCs (seeding density of $4.5x10^4$ cells) (n=4) were seeded on sterile $Hybrid_1$ and $Hybrid_2$ scaffolds (with or without Collagen I coating) and incubated for 12 hours to ensure static attachment. Media was added and changed every 2 to 3 days. After 24 hours, samples were gently washed with PBS and a solution containing fresh medium with 10% of Alamar Blue reagent was added. Samples were allowed to incubate for 8 hours, then 100µL of the samples was transferred to a 96-well plate and absorbance was measured at 570 nm with 600 nm as a reference.

3.3 Results

3.3.1 Successful fabrication of bead-free coaxial fibrous scaffolds

The coaxial electrospinning method was used to fabricate biomimetic substrates to serve as a potential nail splint in future in vivo studies (**Figure 12A**). Engineering a biocompatible nail splint requires the fabrication of a porous yet durable substrate capable of protecting the injured nail bed without causing further damage during healing stages. The material would also need to separate the interaction between the proximal nail fold and underlying matrix soft tissue to prevent

tissue fusion and thereby hindering the nail plate to smoothly grow distally. Poly(lactide-*co*-glycolide) (85:15) and gelatin were used in the study to combine features such as mechanical strength and tailorable degradation rate of the former and the cell preferred hydrophilic properties of the latter. Optimal parameters for the coaxial electrospinning process yielded bead-free uniform $Hybrid_1$ (10% w/v PLGA-shell, 4% w/v gelatin-core) and $Hybrid_2$ (11% w/v gelatin-shell, 10% w/v PLGA-core) fibers with average diameters ranging 540 nm and 2215 nm, respectively (**Figure 12B-E**).

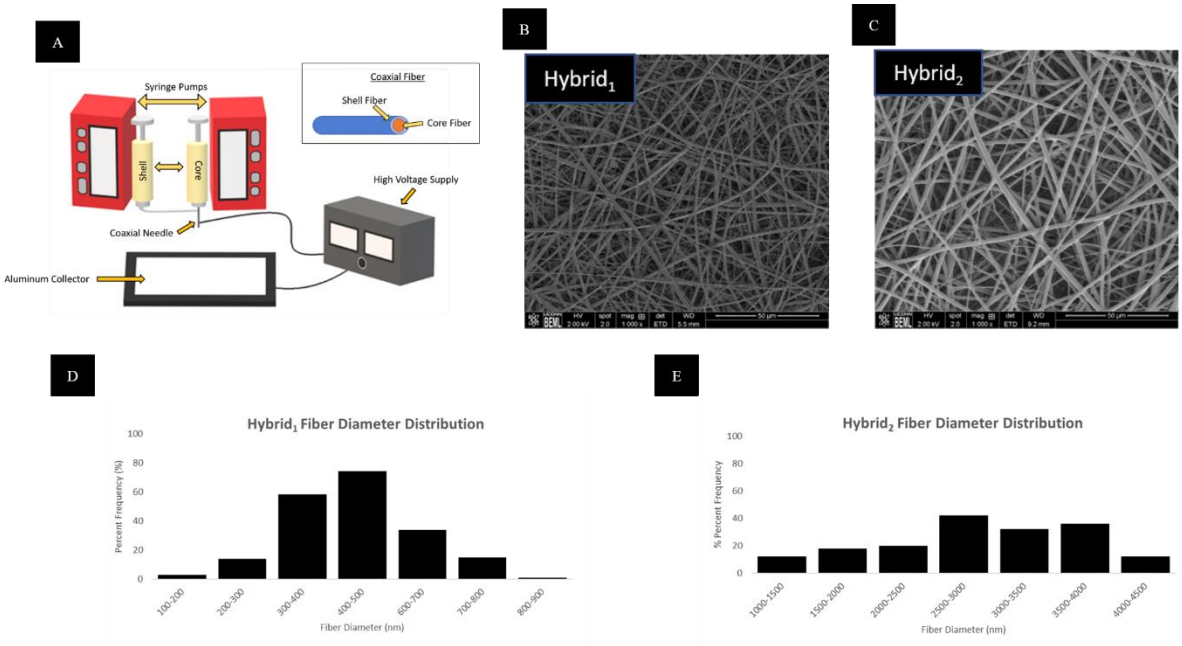

Figure 12. Fabrication of $Hybrid_1$ and $Hybrid_2$ Coaxial Electrospun Scaffolds. **A**. Schematic of coaxial electrospinning setup used to create Hybrid1 and $Hybrid_2$ fibrous scaffolds. Illustrated by Aundrya B. Montgomery. **B.** and **C.** SEM image of $Hybrid_1$ and $Hybrid_2$ optimized coaxial electrospun fibrous scaffolds, respectively. **D**. $Hybrid_1$ diameter distribution histogram displaying fiber diameters ranging between 227-792 nm. **E**. Fiber diameters ranging from 205-4938 nm are observed in $Hybrid_2$ coaxial scaffolds.

3.3.2 Confirmation of core-shell fiber encapsulation

To confirm the presence of core fibers, TEM imaging was used to view the core of $Hybrid_1$ and $Hybrid_2$ scaffolds. Light and dark phases in the TEM images assist us with differentiating the shell fibers from the core. We were able to confirm that our parameters yield encapsulated fibers (Figure **13A&C**), and furthermore, we also compared the concentration of $gelatin^{FTIC}$ in $Hybrid_1$ and $Hybrid_2$ scaffolds to observe encapsulation as well (**Figure 13B&D**). A noticeable difference in the fluorescent intensity of the gelatin can be attributed to two things, the PLGA shell in $Hybrid_1$ encapsulates the gelatin, therefore only faint FITC expression was expected and $Hybrid_2$ has gelatin as the shell and the concentration was increased as well.

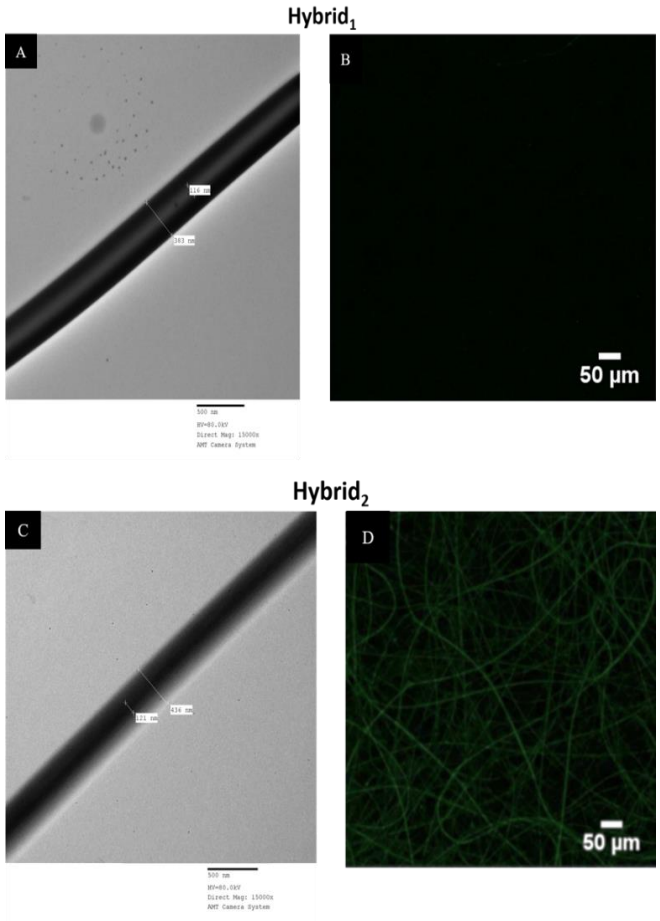

Figure 13. Visualizing encapsulation of Hybrid$_1$ and Hybrid$_2$ core-fibers. **A**. TEM images of Hybrid$_1$ fiber shows core fiber (light contrast, 116 nm) and shell fiber (dark contrast, 383 nm). **B**. Faint FITC signal is consistent with small concentration of gelatin (4% w/v) encapsulated by a shell fiber of 10% w/v PLGA in Hybrid$_1$ scaffolds. **C**. PLGA (dark contrast, 121 nm) is seen within the shell gelatin^{FITC} fibers (light contrast, 436 nm). **D**. Gelatin^{FITC} shell fibers show greater intensity of FITC in Hybrid$_2$ fibers.

3.3.3 Cross-linking Hybrid$_2$ fibers using GA Vapors

Gelatin has been found to enhance the bioactivity of fibrous scaffolds, however, its disadvantages such as hydrophilicity and low mechanical stability require crosslinking procedures to increase gelatin's stability in solution. One of the most widely used and convenient techniques to crosslink collagen-based materials uses glutaraldehyde vapors to enhance properties of the material.[74] To optimize time and GA concentration required to crosslink Hybrid$_2$ scaffolds, 0, 5, 15, and 25% GA solutions were prepared and fiber mats were exposed to the vapors for 1 hours at 37^{o}C (**Figure 14A**). SEM imaging revealed uniformed fibrous mats (**Figure 14B**), and furthermore, fiber diameter was analyzed using ImageJ and results show that there is an inverse relationship between fiber diameter and GA concentration (**Figure 14C**). At 25% GA, average fiber diameters decreased to 1599 nm showing that the PLGA and gelatin were successfully cross-linked in some fashion (**Figure 14D**).

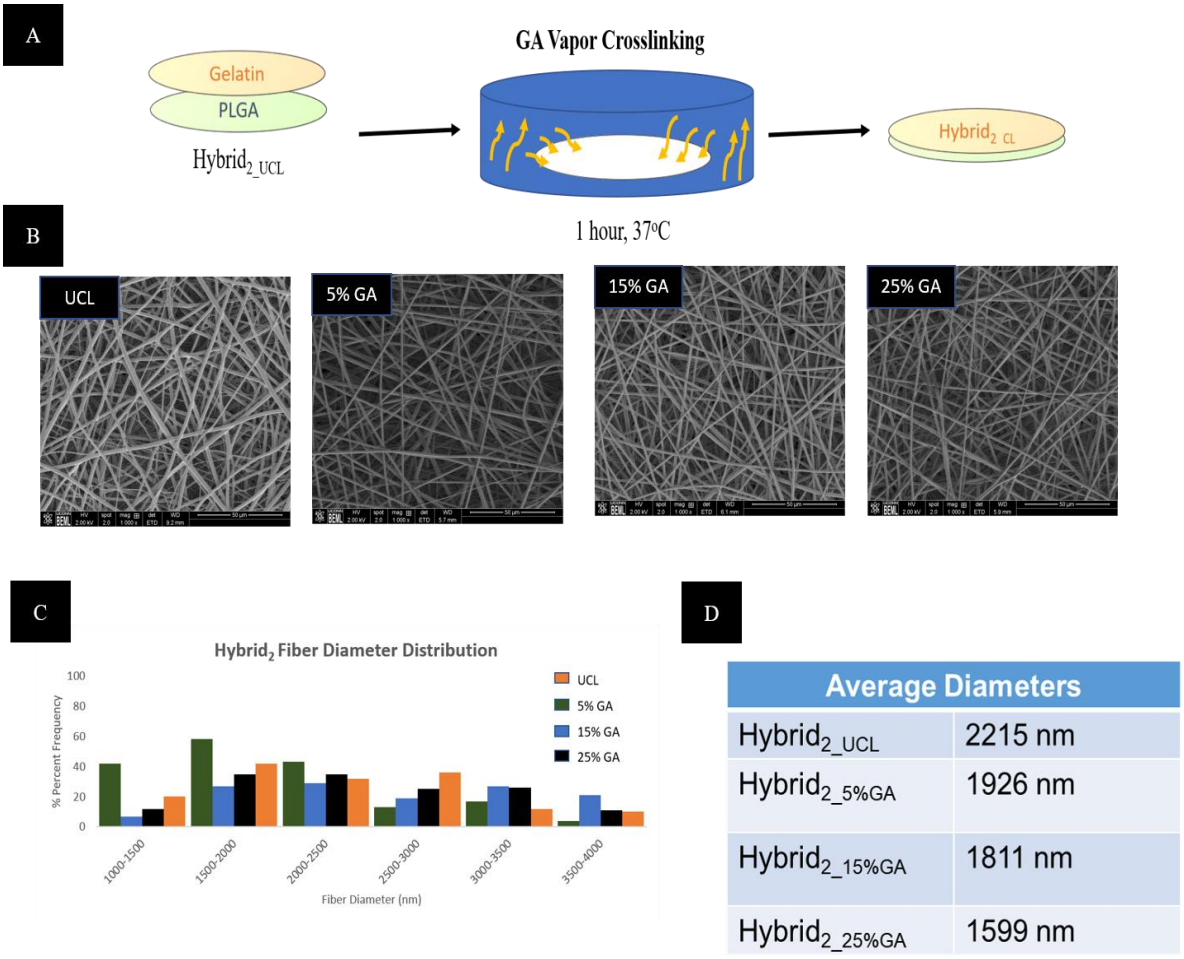

Average Diameters	
$Hybrid_{2\_UCL}$	2215 nm
$Hybrid_{2\_5\%GA}$	1926 nm
$Hybrid_{2\_15\%GA}$	1811 nm
$Hybrid_{2\_25\%GA}$	1599 nm

Figure 14. GA Vapor Crosslinking $Hybrid_2$ fibrous scaffolds. A. Process of crosslinking 11% gelatin and 10% PLGA $Hybrid_2$ coaxial fibrous scaffolds. **B**. SEM images showing the morphology of $Hybrid_{2\_UCL}$ scaffolds and $Hybrid_2$ scaffolds crosslinked with different GA concentrations. **C**. Fiber diameter distribution of fibers crosslinked with 0, 5, 15, and 25% GA concentrations. **D**. Average diameters of $Hybrid_2$ scaffolds show a decrease as the concentration of GA increases.

3.3.4 Measuring the hydrophilic potential of hybrid scaffold

To evaluate the potential of the hybrid scaffolds to retain water, which can have an effect on the behavior of the material *in vivo*, we submerged $Hybrid_1$, $Hybrid_{2\_UCL}$, and $Hybrid_{2\_CL}$ scaffolds in EpiLife standard media to mock *in vitro* conditions to observe the swelling of the materials over 1, 3, and 7 days. SEM images reveal that compared to UCL groups, $Hybrid_{2\_CL}$ fibers did not hold their morphology due to increased water intake (**Figure 15A**). This is understandable due to the hydrophilic nature of the gelatin shell solution. $Hybrid_1$ and $Hybrid_{2\_UCL}$ scaffolds held fiber morphology for up to 7 days in culture. This can be attributed to the hydrophobicity properties of PLGA and also, when gelatin composes the shell of the fiber and is not cross-linked to the PLGA core fiber, the hydrophilicity of the gelatin will cause it to dissolve in the aqueous solution. The percentage of swelling of $Hybrid_1$, $Hybrid_{2\_UCL}$, and $Hybrid_{2\_CL}$ scaffolds when in aqueous solution further confirmed a significant increase of $Hybrid_{2\_CL}$ fibers when compared to hydrophobic UCL groups (**Figure 15B**).

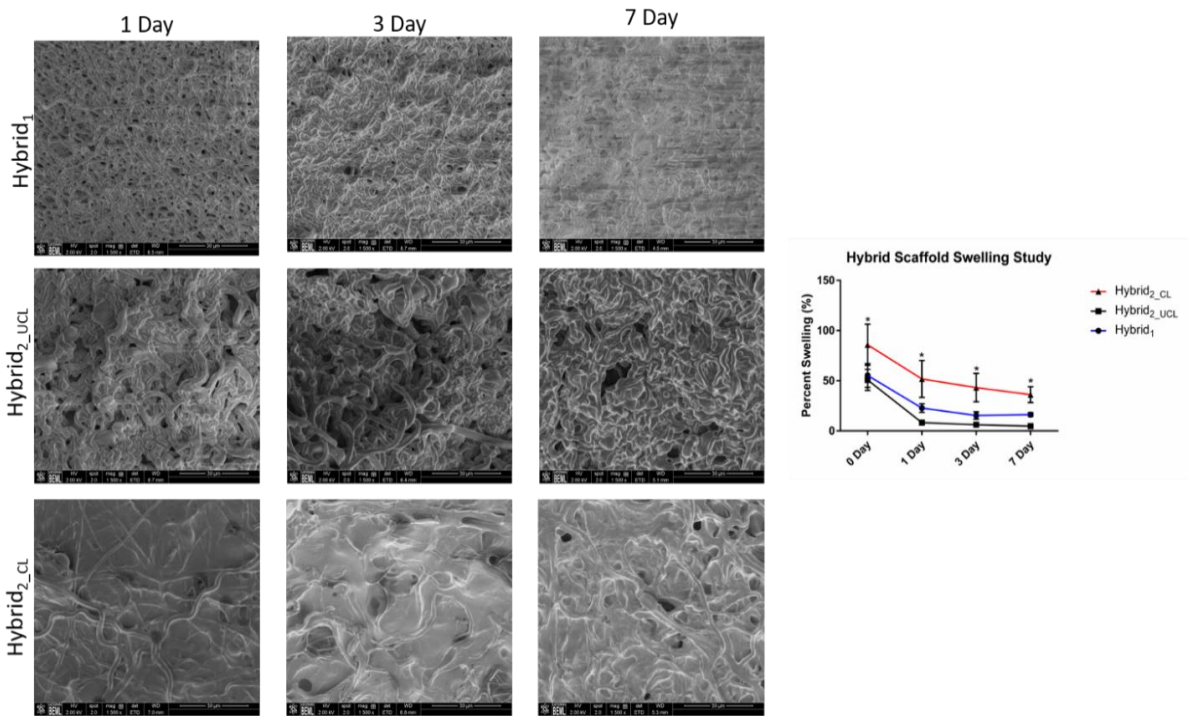

Figure 15. Swelling properties of Hybrid$_1$, Hybrid$_{2_UCL}$, Hybrid$_{2_CL}$ scaffolds. **A**. SEM images of Hybrid$_1$, Hybrid$_{2_UCL}$, Hybrid$_{2_CL}$ scaffolds after 1, 3, and 7 days of exposure to EpiLife media. **B**. Hybrid$_{2_CL}$ shows a significant increase in swelling over the course of 7 days when compared to Hybrid$_1$ and Hybrid2$_{_UCL}$ groups.

3.3.5 NSC attachment and viability on hybrid scaffolds

To confirm if gelatin shell fibers induced cell attachment better than PLGA shell scaffolds, NSCs were seeded on the fibrous substrates and cell attachment was observed using fluorescent and crystal violet staining mechanisms. Between Hybrid$_1$ and Hybrid$_2$ scaffolds, we observed low cell attachment at early time points, however, we start to see NSCs migrate and spread on fibrous substrates at 12 hours and by 24 hours, a noticeable increase in actin staining suggesting an increase in NSC attachment to both substrates (**Figure 16**). Moreover, crystal violet results suggests that Hybrid$_2$ fibers induced cell attachment better than Hybrid$_1$ scaffolds over a 24 hour period (**Figured 17**). By 24 hours, there is a significant difference between NSC attachment to

Hybrid$_1$ and Hybrid$_2$ scaffolds ($p<0.0001$****) which is expected due to interaction with favored hydrophilic interactions. NSCs remain viable after 24 hours on hybrid scaffolds. No significance is noted between groups **(Figure 18**).

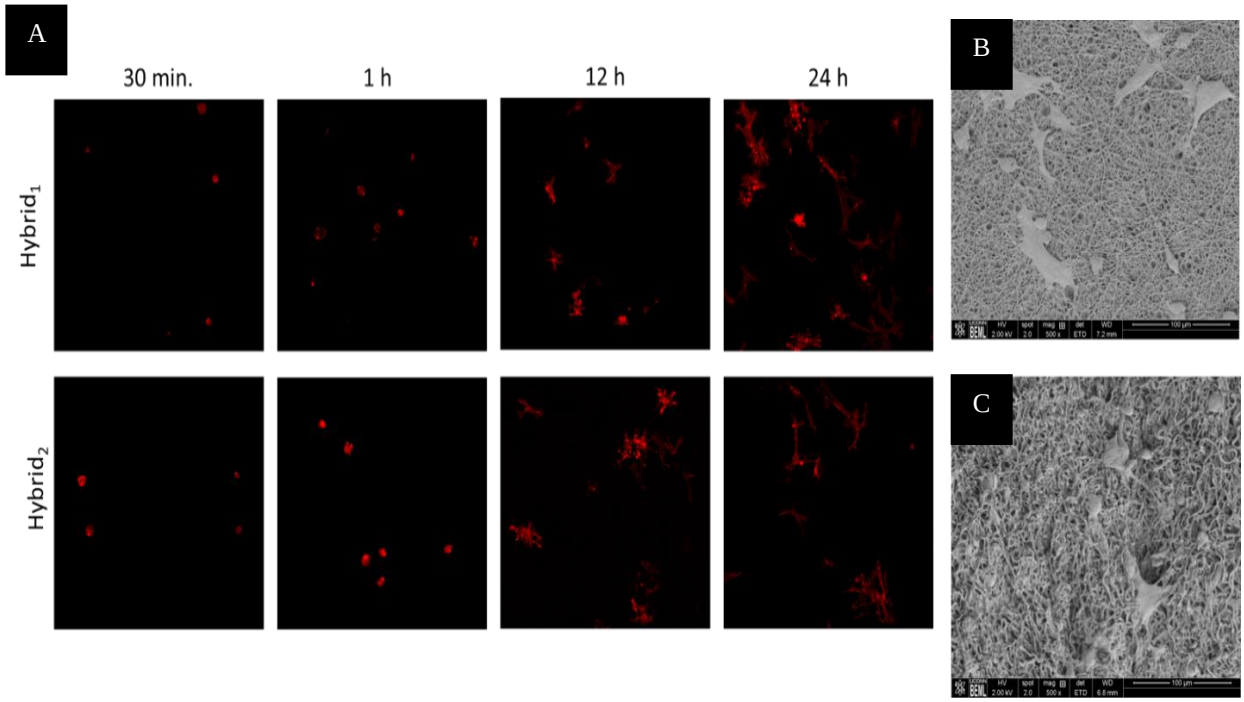

Figure 16. Observing NSC Attachment on Hybrid$_1$ and Hybrid$_2$ scaffolds. A. Phalloidin (actin=red) staining of NSCs seeded on Hybrid$_1$ and Hybrid$_2$ scaffolds at 30 minutes (min), 1 hour (h), 12 h, and 24 h. **B-C**. SEM images of NSCs seeded on Hybrid$_1$ and Hybrid$_2$ scaffolds respectively after 24 h.

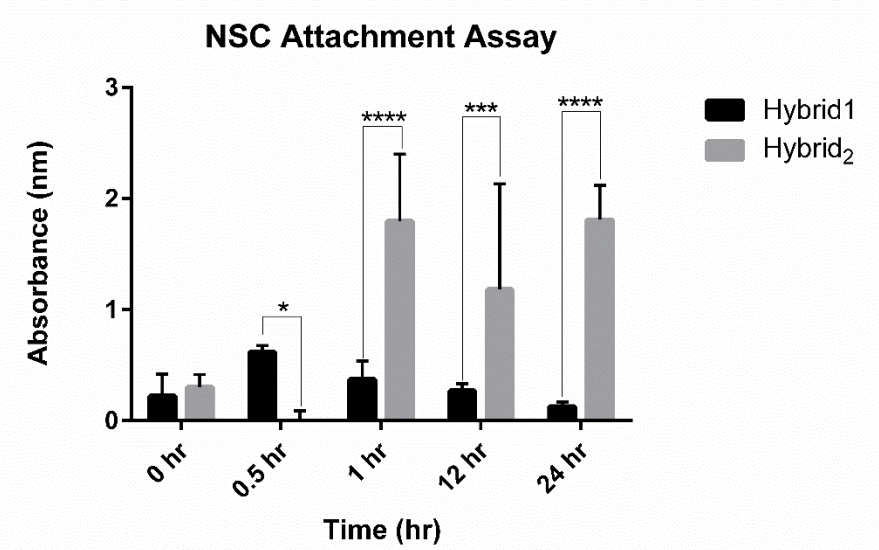

Figure 17. Quantification of NSC Attachment via Crystal Violet Assay. NSCs show significant increase (****$p<0.001$) in $Hybrid_2$ attachment between 0.5 hr-24 hr time points when compared to NSCs that attached to $Hybrid_1$ scaffolds.

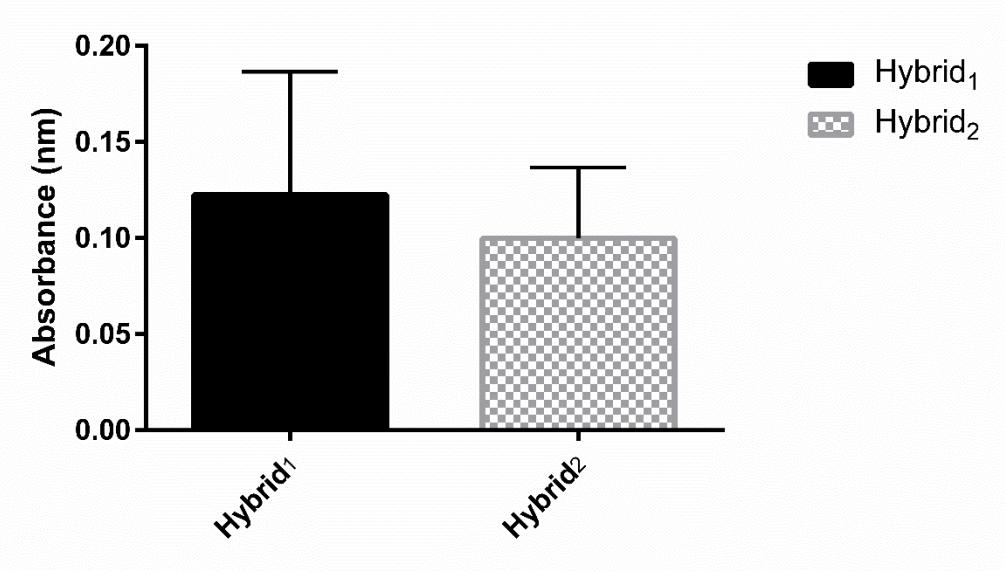

Figure 18. NSC metabolic activity observed using Alamar Blue Viability Assay. NSCs remain viable after 24 hours on hybrid scaffolds. No significance is noted between the two groups.

Chapter 4: Observing the Efficacy of Hybrid$_2$ NSC Loaded Matrices in Rat Model of Non-Regenerative Nail Injury

4.1 Introduction

To date, the regeneration of a fingernail has not been completed. A study conducted by Okamoto et al. evaluated the potential of cells from the nail matrix along with skin and nail fibroblast cells to produce a hard-keratinized nail plate in an *in vivo* subcutaneous rat model. The authors found that their implants, composed of nail matrix cells and nail fibroblasts combined with a collagen gel matrix produced hard keratin and can survive *in vivo*.[55] Recently, nail bed decellularized matrices were evaluated in hopes of regenerating nail tissue, and results revealed the potential of the bioactive system, functionalized using bone marrow stem cells to express epithelial stem cell markers *in vivo*.[75] While these studies support claims that NSCs can be successfully implanted, in both studies, the implants were not placed in the correct anatomical position of the nail matrix. To date, only subcutaneous models have been attempted to evaluate the efficacy of cell delivery systems in efforts to generate hard nail tissue. Multiple reasons, such as the implant site and extracellular environment, could attribute to disadvantages faced with the previously stated systems. Taking this into consideration, for the first time we have developed a rat animal model that ablates the nail matrix to further evaluate regenerative engineering strategies in rescuing cases similar to those treated in the clinic.

4.2 Materials and Methods

4.2.1 Materials

RNU rats were purchased from Charles River Laboratories, (Wilmington, MA) and F344-Tg(UBC-EGFP)F455Rrrc rats were obtained from the Rat Resource & Research Center (Colombia, MO). All animal handling and procedures were carried out in accordance with the Institutional Animal Care and Use Committee at the University of Connecticut Health Center,

Farmington, CT. Phenol EZ swabs were purchased from Medline Industries, Inc. (Northfield, IL). 6-0 prolene sutures were purchased from Fisher Scientific (Hampton, NH).

4.2.2 Methods

4.2.2.1 Phenol ablation of the nail matrix

Male RNU rats (6-8 week old) were anesthetized and subjected to phenol chemical matricectomy on the right hindpaw (digits 2nd-4th). Briefly, the proximal nail fold was separated from the underlying tissue to reveal the nail matrix region. Phenol was applied to ablate the nail matrix region and then neutralized using 70% isopropyl alcohol. The left paw was subjected to nail avulsion without phenol application and used for control. Animals were euthanized 2 and 4-weeks later and digits were harvested and sent to histology for further analysis. Whole mount images of the digit tips were taken using a light microscope and Leica program (12.5X).

4.2.2.2 NSC^{GFP+} delivery system implantation

Nail matrix tissue was isolated from male F344-Tg(UBC-EGFP)F455Rrrc rats and used for explant culture. Briefly, once tissue was harvested, it was washed three times with PBS then allowed to attach to a T-25 flask coated with collagen I for 4 hours before adding EpiLife media containing 10% FBS and 1% P/S. NSCs were removed from flasks using accutase solutions and seeded at $1.0x10^5$ cells per scaffold (sterilized prior to seeding using the same methods as reported in Chapter 4) for *in vivo* implant experiments.

4.2.2.3 In vivo delivery of NSC^{GFP+} fibrous matrix

RNU rats (6-8 weeks old) underwent phenol ablation on both right and left hindpaws (digits 2^{nd}-4^{th}). The nail organ was allowed to heal for 3 weeks before implant procedure. Hybrid delivery systems containing GFP^+NSCs were implanted in the nail matrix region of the 2nd-4th right hindpaw digits and Hybrid scaffolds without GFP cells were implanted in the matrix regions on

the left hindpaw and used as control. After 2 and 4 weeks, host animals were euthanized and tissue was sent to histology for analysis.

4.2 Results

4.2.1 Establishing a rat model of non-regenerative nail injury

Traumatic nail injuries, such as crush injuries, lacerations, and avulsions, all have one thing in common—if the nail bed and/or the nail matrix is not promptly and meticulously treated, the prognosis will often favor the regeneration of a dysmorphic nail plate. Strategies to develop an animal model to mimic nail injuries seen in the clinic must impair the function of the nail matrix, and the nail bed itself to directly affect the smooth outward growth of the nail. Taking this into consideration, we used a chemical matricectomy procedure, commonly used by podiatrists in ingrown toenail cases to permanently destroy or ablate the nail matrix.[76] We compared control groups, nail avulsion, with those who underwent phenol ablation and observed outward growth of the nail plate of nail avulsed animals by 4 weeks. However, those who experience phenol ablation showed decreased growth of the nail plate as seen in whole mount images (**Figure 19**). H&E images suggest the presence of regenerated keratinized nail tissue in both 2 and 4-week avulsed groups, however, in animal digits that were subjected to phenol ablation, the region where keratinized nail tissue is normally located show noticeable deformities and a decrease in nail plate tissue (**Figure 20**). Nail regeneration remained absent in phenol ablated samples at 6 weeks, but in avulsed animals, noticeable nail regeneration was observed. Lgr6 expression is present in the nail matrices of the avulsed animals at 6 weeks, however, the expression of the NSC related protein is no longer observed after phenol ablation (**Figure 21**). When compared to regenerative competent avulsed samples, there is a significant decrease in outward growth of the nail plate noticed in 2, 4, and 6 week ablated groups (**Figure 22**). These results suggest that we have

established a method that yields a non-regenerative phenotype of the nail organ and could further be used to evaluate the potential of our NSC delivery system in rescuing the regeneration of the nail.

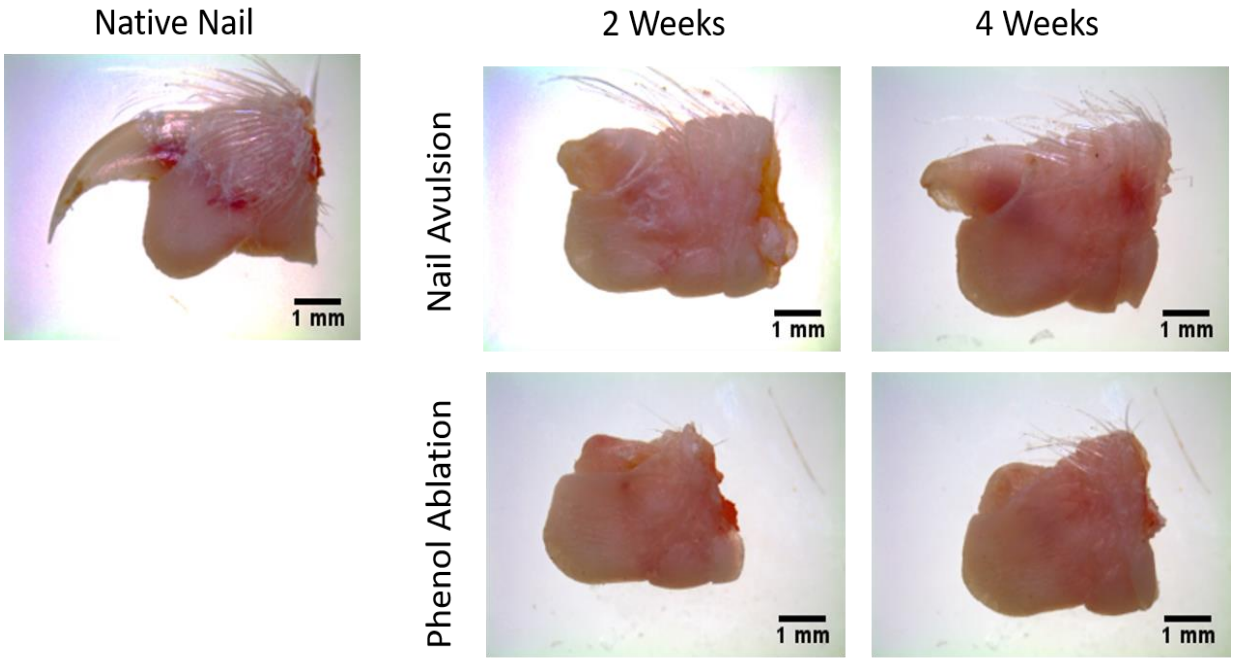

Figure 19. Whole mount imaging of *in vivo* nail avulsion and phenol ablation groups. 2 and 4-week avulsed groups show noticeable regeneration of the nail plate compared to groups that were subjected to phenol ablation. (n=5 animals; 30 digits per sample)

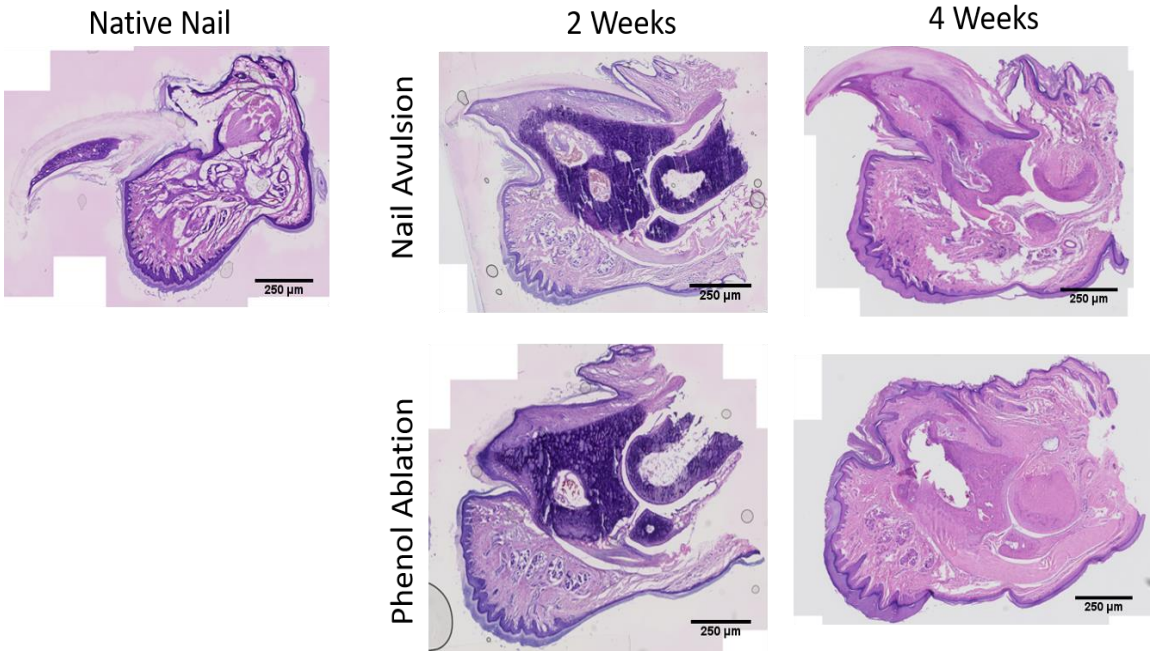

Figure 20. H&E staining of nail avulsion and phenol ablation 2 and 4-week groups. Nail outward growth is noticeably precluded as a result of phenol ablation when compared to avulsed groups. At 4 weeks, the nail plate is present, but no visible in phenol treated nail organs.

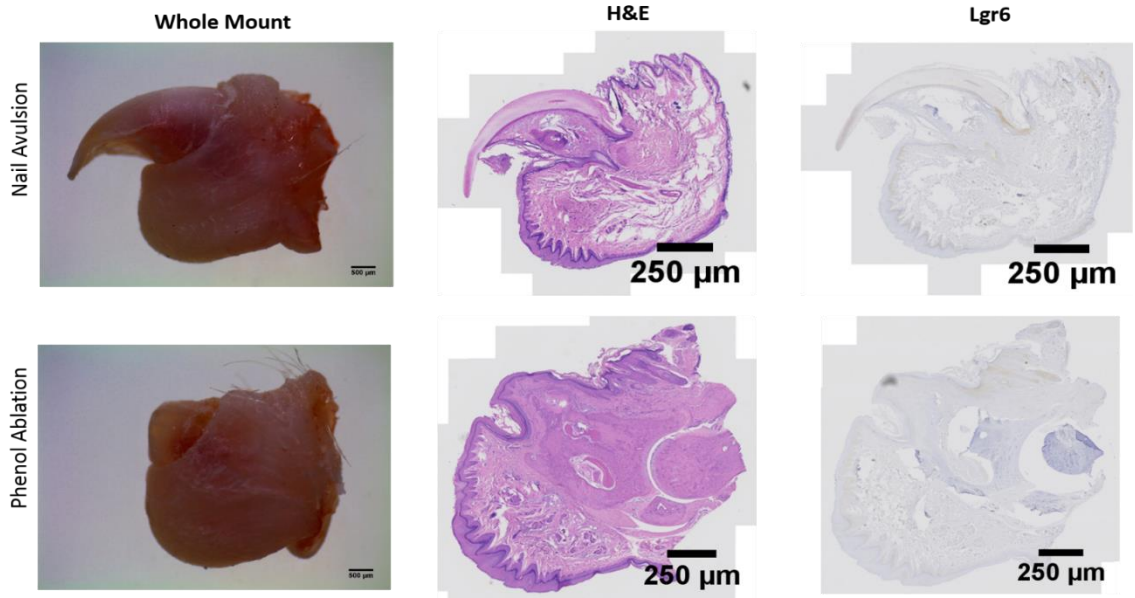

Figure 21. 6 week post-operative nail avulsion and phenol ablation. Whole mount images show decrease in outward nail growth after phenol ablation. H&E staining show the hard nail plate in avulsed rat digits, but is absent in ablated samples. Lgr6 expression is found in the nail matrix region of avulsed digits, but expression decreases after phenol ablation.

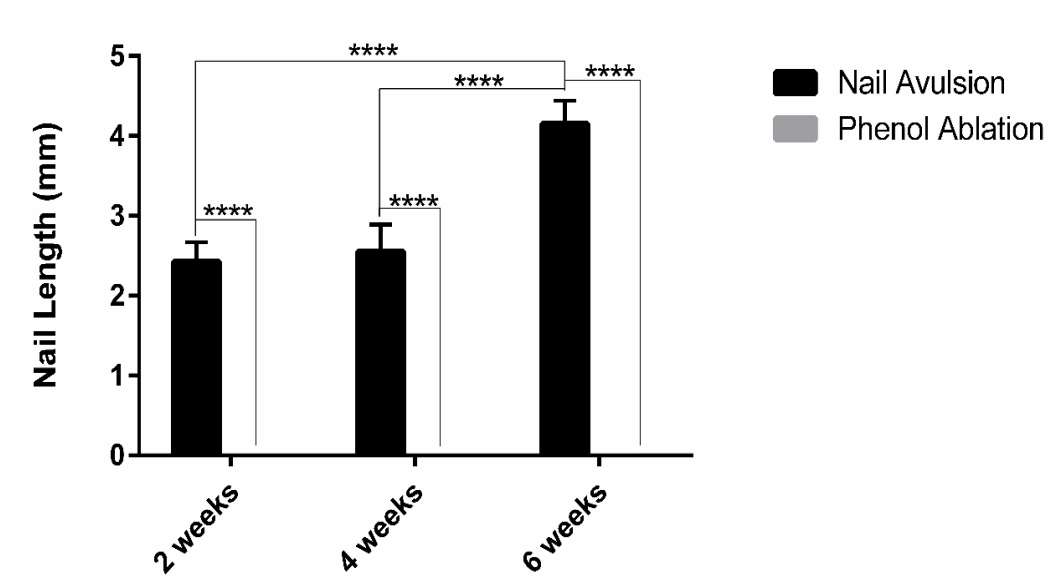

Figure 22. Outward nail growth of 2,4, and 6-week avulsed and phenol ablated treatment groups. ImageJ analysis was used to measure the outward growth of the nail plate for 2, 4, and 6-week time points. When compared to the nail length of the avulsed digits, a significant decrease ($p<0.0001$***) was observed in the phenol ablated groups, even at 6 weeks (2 and 4 weeks n=5 animals, 15 digits per sample; 6 weeks n=3 animals; 9 digits per sample).

4.2.2 In vivo nail matrix implantation of NSC loaded hybrid scaffold

Once our ablation procedure was seen to impede outward nail growth, we wanted to next test the efficacy of our hybrid scaffold system *in vivo.* First, we ablated the nail matrices on the left and right hindlimb digits (2^{nd}-4^{th}). Once ablated, the animals (n=5; 15 digits per sample) were allowed to heal for 3 weeks post ablation. After 3 weeks, animals were subjected to NSC^{GFP+} $hybrid_2$ implants (treatment group) or $hybrid_2$ implant alone (control) (**Figure 23**). After 2 and 4 weeks, animals were euthanized and whole mount images revealed a noticeable difference between native nail tissue when compared to the control and treated implant groups (**Figure 24**). ImageJ data showed a significant decrease in nail growth of both scaffold and NSC^{GFP+} implants when compared to avulsed groups at 2 and 4 weeks post implantation ($p<0.0001$****) (**Figure 25**). H&E staining is consistent with the previously stated results in that there is not a noticeable out growth

from the proximal matrix of hard nail tissue (**Figure 26**). To measure the rescue potential of our implants, we compared the nail length of the phenol ablated groups to NSC^{GFP+} implant scaffolds and hybrid scaffolds without cells. A significant decrease in nail length is observed between the scaffold alone and phenol ablated groups ($p<0.01$*) (**Figure 27**).

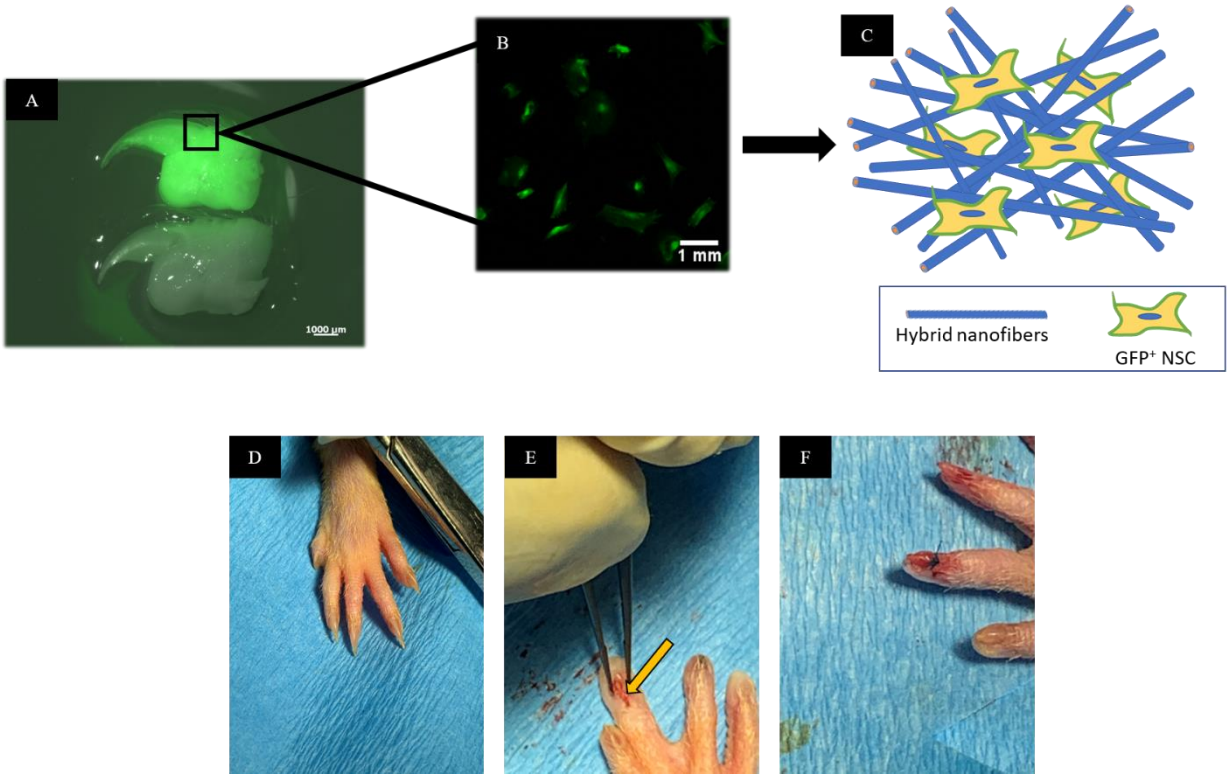

Figure 23. GFP^+ NSC isolation and implant procedure. A. Ubiquitous EGFP expression rat F344-Tg(UBC-EGFP)F455Rrrc used for tissue isolation and explant NSC culture. **B**. $EGFP^+$ cells used for NSC^{GFP+} implant. **C**. Schematic of implant scaffold seeded with GFP^+ cells for 2 and 4-weeks. **D**. Tourniquet is applied before avulsing the nail. **E**. Implant site for fibrous matrices. G. 6-0 prolene sutures to close wound. (n=9 animals; 54 digits)

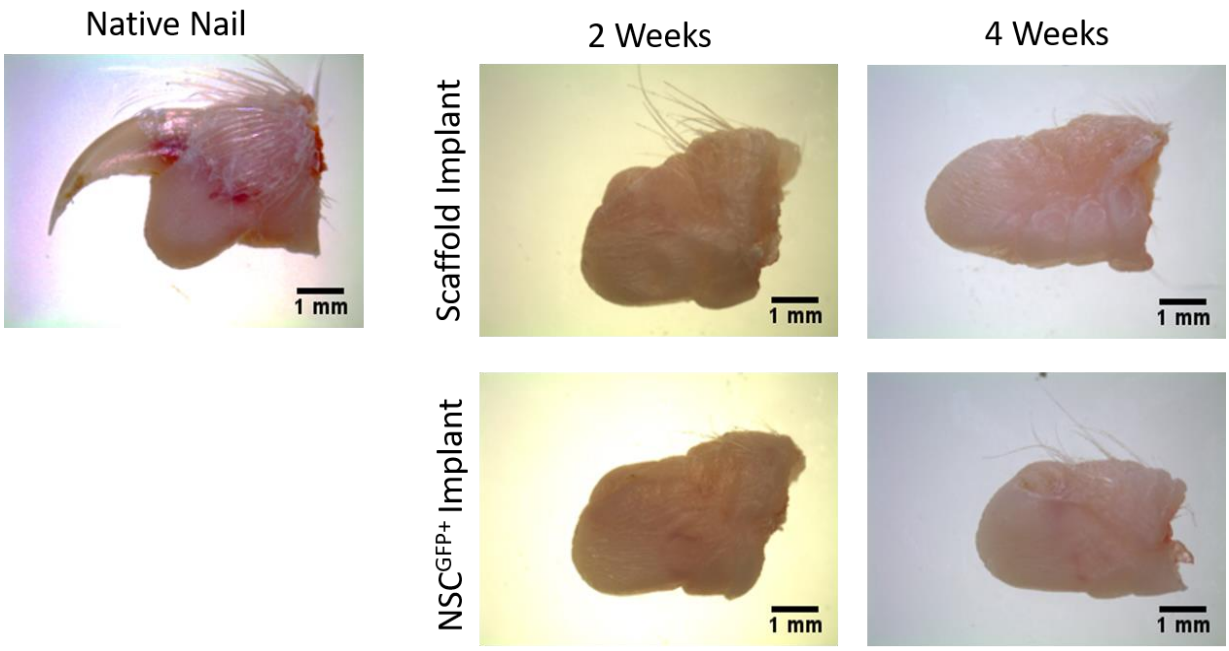

Figure 24. Whole mount imaging of 2 and 4-week hybrid scaffold and NSC^{GFP+} implant. At 2 and 4 weeks, scaffold and NSC^{GFP+} implants do not show outward nail plate growth when compared to native nail tissue. (n=4 animals, 12 digits)

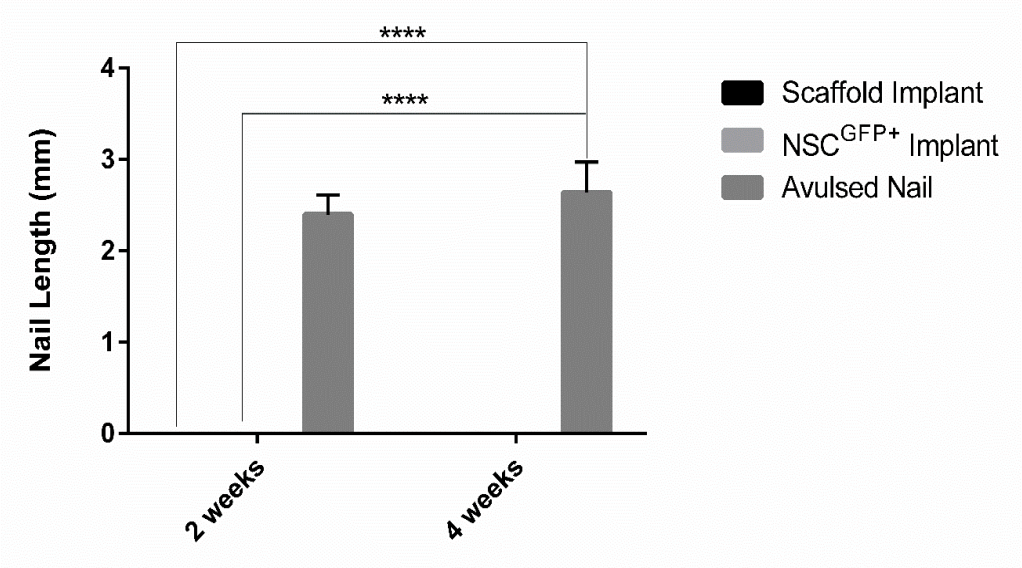

Figure 25. Nail growth post implantation of Hybrid scaffolds and NSC^{GFP+} implant. ImageJ analysis of the outward growth of the nail plate in NSC^{GFP+} implant and scaffold implant groups. Results show a significant decrease in both NSC^{GFP+} implant and scaffold implant outward nail growth when compared to native nail tissue ($p<0.0001$****). No significance is found between implant groups. (n=4 animals, 12 digits).

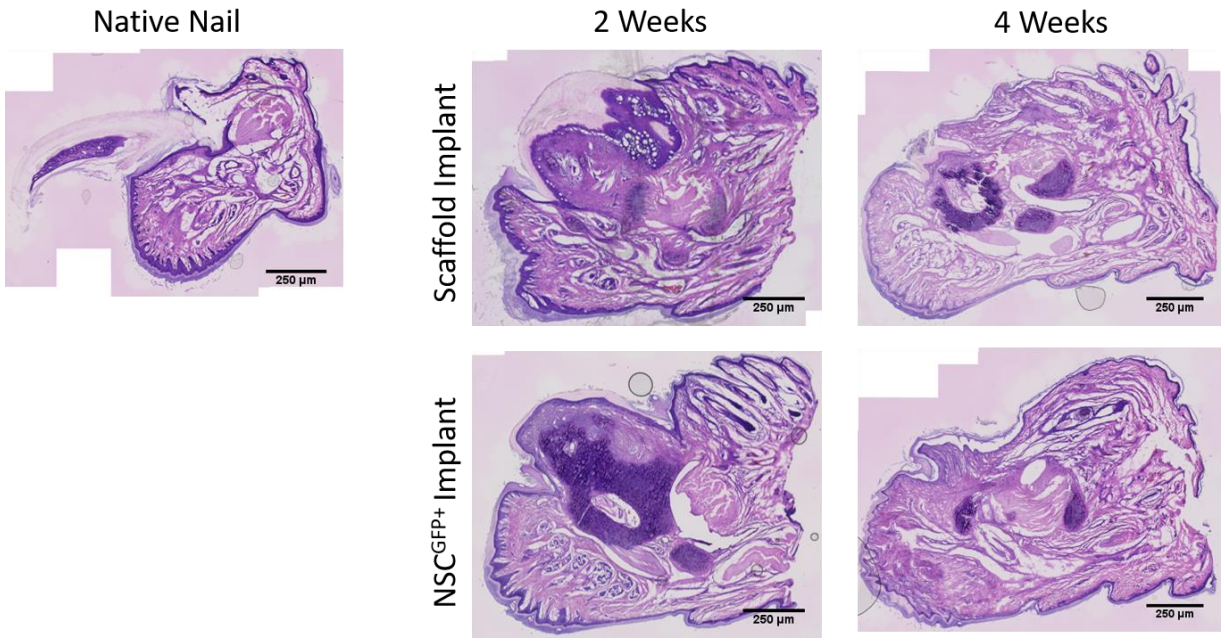

Figure 26. H&E imaging of scaffold and GFP$^+$ implant groups 2 and 4 weeks. Tissue sectioning shows a noticeable difference in the nail plate region of both scaffold implant and NSC^{GFP+} implant groups when compared to the native nail digit.

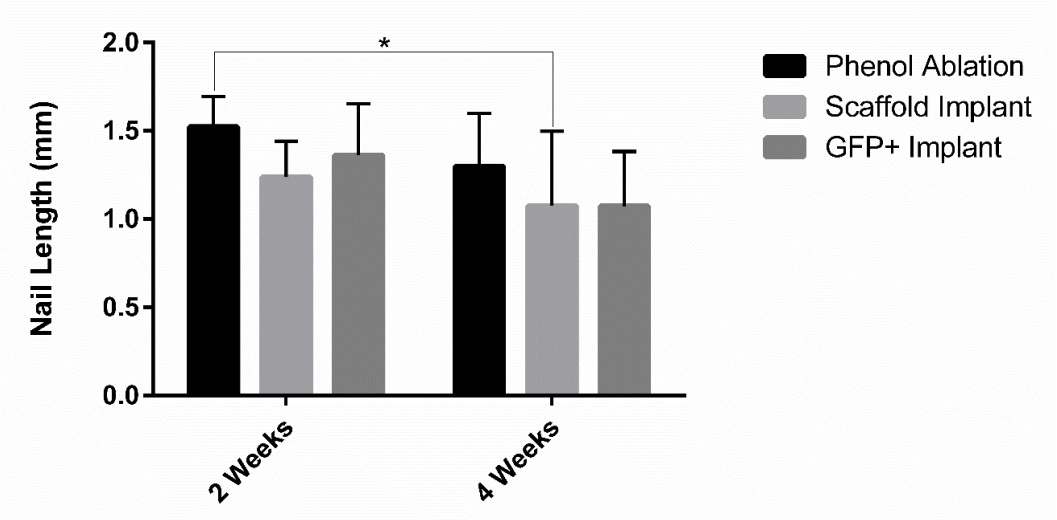

Figure 27. Observing the efficacy of Hybrid scaffold implant and NSC^{GFP+} in recovering nail growth. When compared to phenol ablation, the scaffold implant alone showed a significant decrease in outward nail growth. ($p<0.01$*). No significance is noted between the growth of NSC^{GFP+} implants in either 2 or 4 week time periods.

4.3 Discussion and Future Direction

Acute traumatic nail injuries are often coupled with a prognosis that is uncertain of whether the regenerated tissue will fully resemble its function and aesthetic appearance before injury. In efforts to develop methods to apply to nail traumatic injury cases, we established a rat model that displays a non-regenerative phenotype of nail injury, which has not currently been established in the field. This is exciting in which now methods to address nail traumas can be localized to the correct anatomical position, while previous studies have only studied methods in subcutaneous models. This model is advantageous as well in terms of developing methods for clinical translation due to it mimicking what emergency room and primary physicians commonly see in the field. Having a realistic region to implant bioengineered scaffolds allows us to monitor behavior of these materials and test their efficacy of promoting favorable nail regeneration *in vivo*. The focus of the study was to develop a biomimetic matrix that is capable of transporting the scaffold system to the nail matrix and improve the regeneration of the hard nail plate. This proof-of-concept study revealed the effectiveness of phenol to impair nail plate growth, however, multiple challenges during the surgical procedure and post operation could be attributing factors to the absence of nail growth in the scaffold and NSC^{GFP+} implant groups.

The surgical procedures conducted in the study were challenging to complete due to the small size of the rat nail matrix. This also led to other downstream challenges such as correct location of phenol and the placement of the scaffold. Phenol caused necrosis to the small region of the nail matrix and could have possibly affected other areas of the nail such as the nail bed and proximal nail fold tissues, causing further damage to the digit tip overtime. During the first implant procedure (3 days post ablation) we attempted the second procedure to implant the materials into the nail matrix, but unfortunately the tissue was completely edematous and fragile causing an

inability to implant the scaffold into the matrix region (**Figure 28**). We then allowed the animals to heal for 3 weeks prior to attempting the second implant procedure and found that at 3 weeks, the nail organs of the animals were completely healed, and no sign of outward nail growth was noted at that time.

Figure 28. Scaffold implant attempt 3 days post phenol ablation. First implant procedure was attempted 3 days post phenol ablation, however, scaffolds were unable to be secured in the matrix region due to edematous and fragile tissue at implant site.

Other challenges seen included incorrect placement of the scaffold. Fibrous substrates, even when prepared at mm x mm dimensions were still too large for the implant pocket site. This cause extra manipulation of the matrix upon implantation and incorrect placement of the scaffold more proximal to the nail matrix region. In addition to the implant site challenges, the behavior of the animal, (i.e., wound site chewing), could have eliminated the scaffold prior to the harvest periods. The possibility of suture placement impairing nail growth is a possible reason of an absence of regeneration as well. In the clinic, nail splints are inserted between the nail matrix and

the nail fold with part of the material located in the external environment, however, we were unable to splint the nail as seen in humans. This was mainly due to the small area of the region of interest, the risk of animals removing the scaffold by biting or other methods of mechanical movement.

The inability of our regenerative engineered matrix to rescue the nail matrix region suggests that aggressive nail matrix injuries, such as a chemical burn, will not yield the regeneration of a nail plate. Furthermore, we believe that the development of a more subcritical animal model would aid in future elucidation of how bioengineered nail matrices could assist with hard nail plate regeneration. Patients with both acute and chronic nail injuries, most often, do not have a completely ablated nail matrix as seen in our phenol ablation model. Thus, creating animal models that introduce traumatic injuries without ridding the nail organ of its matrix will assist with future *in vivo* studies geared toward strategies to rescue cosmetic appearance of injured nail organs.

Chapter 5: Conclusions and Future Works

Overall, we were able to further elucidate the behavior of NSCs *in vitro* and their behavior on electrospun matrices, which currently has not been defined in the literature. Furthermore, we have fabricated a proof-of-concept biomimetic system for applications geared toward traumatic nail injuries and have observed its efficacy in a novel *in vivo* rat model that displays a non-regenerative nail plate phenotype. Evaluating the effect of NSCs in the repair and rescue of trauma to the nail can aid in the development of remedies to apply to these cases in the clinic; moreover, could possibly apply to future regenerative engineering methods focused on mammalian digit regeneration.

While we did not see noticeable regeneration of the nail plate after nail matrix ablation with phenol; however, we were able to establish proof-of-concept that regeneration of the nail can be impaired using similar techniques used in humans. The mechanism behind how phenol causes ablation results in necrosis of the tissue, and due to the small area of the rat nail matrix, unfortunately, we were not able to control specific areas of where the phenol was placed. Future optimization of the model should introduce another method of injury such as physical ablation including lacerations to the nail bed and to the nail matrix to observe the effects on outward nail growth. Also, equipping the fibrous scaffold with molecules to induce NSC proliferation (i.e., Wnt molecules or other factors associated with wound healing) could possibly assist with favorable outcomes of nail regeneration such as aesthetic appearance and function.

Even though we suspect the aggressive nature of the phenol ablation to be the reasoning behind the implant results, we attempted to modify the hybrid scaffolds by protein surface modification. After coating the scaffolds with collagen I, we found that even though NSCs had an increase in attachment to $Hybrid_2$ matrices, NSC metabolic activity showed an increase over 7

days in coated Hybrid$_1$ and Hybrid$_2$ scaffolds, and viability showed no significance between the Hybrid$_1$ uncoated samples (**Figure 29**). In addition to these results, a recent paper published by Yu et al. reported SEM images of the decellularized nail's ECM, which consisted of aligned fibers.[75] In the present study, random electrospun fibers were used, however, to mimic the native ECM, *in vitro* modifications of the fibrous substrate are currently being observed.

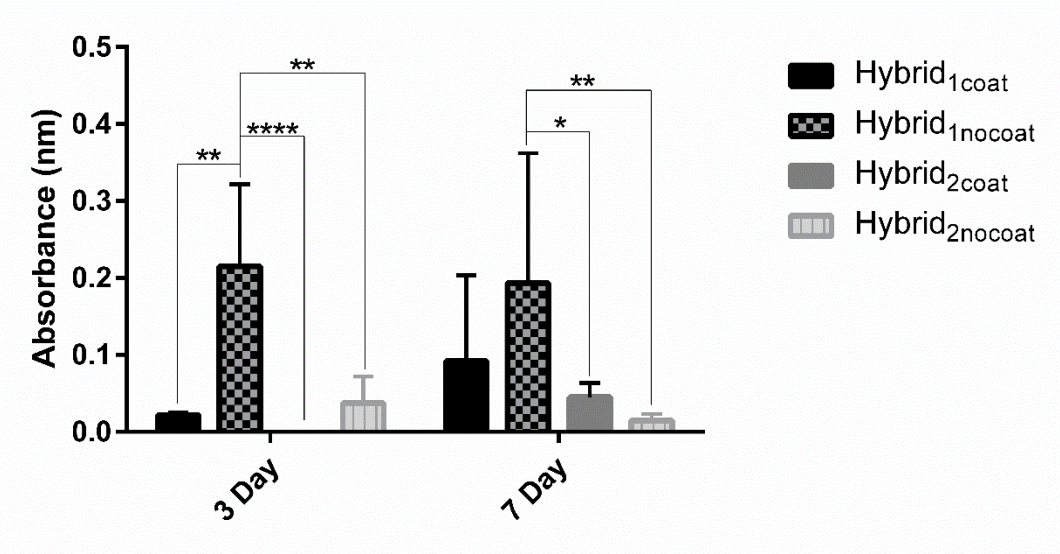

Figure 29. Surface modification effect on NSC metabolic activity. 3 and 7 day analysis of NSC viability on collagen I coated Hybrid$_1$ and Hybrid$_2$ scaffolds. Increase in metabolic activity is noted in Hybrid$_1$ coated scaffolds over 7 days, with no significance noted between uncoated Hybrid$_1$ scaffolds at the same time point. Hybrid$_2$ coated scaffolds show an increase in viability at 7 days. $p<0.01$*, $p<0.001$**, $p<0.0001$***, $p<0.00001$****

Our rat model of establishing non-regenerative nail growth *in vivo* showed promise in terms of nail plate ablation, however, our implant was unsuccessful in rescuing this phenotype. This can be attributed to the aggressive nature of the phenol treatment and suggesting the need for a lesser extreme method (i.e., physical matricectomy and/or fusion of the nail fold tissue to nail matrix region) in order to observe the potential of our engineered fibrous matrix *in vivo*. The current study

has developed a novel animal model specifically designed to mimic a traumatic nail injury and to attempt to rescue nail regeneration using regenerative engineered remedies. Our delivery system reveals a great possibility of the material to be applied to these cases, however, to apply our matrix to a model that mimic injuries most often seen in the clinic (i.e., partially damaged nail matrices and nail beds or chronic traumatic nail injuries), a subcritical model of nail injury is needed. Evaluating the efficacy of our engineered fibrous substrate could prove useful in regenerative engineering a widely applicable nail splint to improve the aesthetic prognosis of nail traumatic injuries.

Chapter 6: References

1. Singal A, Arora R. Nail as a window of systemic diseases. *Indian Dermatol Online J*. 2015;6(2):67-74.

2. Shieh SJ, Cheng TC. Regeneration and repair of human digits and limbs: Fact and fiction. *Regeneration (Oxf)*. 2015;2(4):149-168.

3. Liu Y, Li X, Li R, Zhang J, Lu L. Reconstruction of complex nail matrix defect using the homodigital reverse fasciocutaneous flap. *Medicine (Baltimore)*. 2018;97(44):e12974.

4. Lorea P. Primary care of nail traumas. *Chir Main*. 2013;32(3):129-135.

5. Tos P, Titolo P, Chirila N, Catalano F, Artiaco S. Surgical treatment of acute fingernail injuries. *Journal of Orthopaedics and Traumatology*. 2012;13(2):57-62.

6. Bharathi RR, Bajantri B. Nail bed injuries and deformities of nail. *Indian J Plast Surg*. 2011;44(2):197-202.

7. Flavia Cristina Morone Pinto, Marcia Oliveira. Surgical nail of biopolymer from sugarcane for preservation of the nail bed after avulsion. *Revista Enfermagem Atual*. 2019;87(25).

8. Figueiredo LA, Ribeiro RS, Melo ALB, Lima AL, Terra BB, Ventim FC. Polypropylene prosthesis for the treatment of fingertip injuries. description of surgical technique and results. *Rev Bras Ortop*. 2017;52(6):685-692.

9. OpenStax College. *Anatomy and physiology*. Rice University; 2013.

10. O'Rahilly R, Müller F. *Basic human anatomy: A regional study of human structure.* WB Saunders Company; 1983.

11. Netter FH. *Atlas of human anatomy, professional edition: Including NetterReference. com access with full downloadable image bank.* Elsevier Health Sciences; 2017.

12. Tubiana R, Chamagne P. Functional anatomy of the hand. *Medical Problems of Performing Artists*. 1988;3:83-87.

13. Haneke E. Anatomy, biology, physiology and basic pathology of the nail organ. *Hautarzt*. 2014;65(4):282-290.

14. de Berker D. Nail anatomy. *Clin Dermatol*. 2013;31(5):509-515.

15. De Berker D, André J, Baran R. Nail biology and nail science. *Int J Cosmetic Sci*. 2007;29(4):241-275.

16. Haneke E. Anatomy of the nail unit and the nail biopsy. *, 34, 2*. 2015;34(2):95-100.

17. Pansky B. *Review of medical embryology.* Macmillan New York; 1982.

18. Haneke E. Nail surgery. *Clin Dermatol*. 2013;31(5):516-525.

19. Patel L. Management of simple nail bed lacerations and subungual hematomas in the emergency department. *Pediatr Emerg Care*. 2014;30(10):742-5; quiz 746-8.

20. Hwang E, Park BH, Song SY, Jung HS, Kim CH. Fingertip reconstruction with simultaneous flaps and nail bed grafts following amputation. *J Hand Surg Am*. 2013;38(7):1307-1314.

21. Idone F, Sisti A, Tassinari J, Nisi G. Cooling composite graft for distal finger amputation: A reliable alternative to microsurgery implantation. *In Vivo*. 2016;30(4):501-505.

22. Champagne L, Hustedt JW, Walker R, Wiebelhaus J, Nystrom NA. Digital tip amputations from the perspective of the nail. *Adv Orthop*. 2016;2016:1967192.

23. Silva JB, Gerhardt S. Trauma to the nail complex. *Rev Bras Ortop*. 2014;49(2):111-115.

24. Strauss EJ, Weil WM, Jordan C, Paksima N. A prospective, randomized, controlled trial of 2-octylcyanoacrylate versus suture repair for nail bed injuries. *J Hand Surg Am*. 2008;33(2):250-253.

25. Tos P, Titolo P, Chirila N, Catalano F, Artiaco S. Surgical treatment of acute fingernail injuries. *Journal of Orthopaedics and Traumatology*. 2012;13(2):57-62.

26. Wang W, Yu J, Fan CY, Liu S, Zheng X. Stability of the distal phalanx fracture - A biomechanical study on the importance of the nail and the influence of fixation by crossing kirschner wires. *Clin Biomech (Bristol, Avon)*. 2016;37:137-140.

27. Shepard GH. Treatment of nail bed avulsions with split-thickness nail bed grafts. *J Hand Surg Am*. 1983;8(1):49-54.

28. Pessa JE, Tsai TM, Li Y, Kleinert HE. The repair of nail deformities with the nonvascularized nail bed graft: Indications and results. *J Hand Surg Am*. 1990;15(3):466-470.

29. Yong FC, Teoh LC. Nail bed reconstruction with split-thickness nail bed grafts. *J Hand Surg Br*. 1992;17(2):193-197.

30. Hsieh SC, Chen SL, Chen TM, Cheng TY, Wang HJ. Thin split-thickness toenail bed grafts for avulsed nail bed defects. *Ann Plast Surg*. 2004;52(4):375-379.

31. Lille S, Brown RE, Zook EE, Russell RC. Free nonvascularized composite nail grafts: An institutional experience. *Plast Reconstr Surg*. 2000;105(7):2412-2415.

32. Eberlin KR, Busa K, Bae DS, Waters PM, Labow BI, Taghinia AH. Composite grafting for pediatric fingertip injuries. *Hand (N Y)*. 2015;10(1):28-33.

33. Fiedler DK, Barrett JE, Lourie GM. Nail bed reconstruction using single-layer bovine acellular dermal matrix. *J Hand Surg Am*. 2017;42(1):e67-e74.

34. Raja Sabapathy S, Venkatramani H, Bharathi R, Jayachandran S. Reconstruction of finger tip amputations with advancement flap and free nail bed graft. *J Hand Surg Br*. 2002;27(2):134-138.

35. Hwang E, Park BH, Song SY, Jung HS, Kim CH. Fingertip reconstruction with simultaneous flaps and nail bed grafts following amputation. *J Hand Surg Am*. 2013;38(7):1307-1314.

36. Yang J, Wang T, Yu C, Gu Y, Jia X. Reconstruction of large area defect of the nail bed by cross finger fascial flap combined with split-thickness toe nail bed graft: A new surgical method. *Medicine (Baltimore)*. 2017;96(6):e6048.

37. Lee KJ, Kim YW, Kim JS, Roh SY, Lee DC. Nail bed defect reconstruction using a thenar fascial flap and subsequent nail bed grafting. *Arch Plast Surg*. 2019;46(1):57-62.

38. Komatsu S, TAMAI S. Successful replantation of a completely cut-off thumb. *Plast Reconstr Surg*. 1968;42(4):374-377.

39. Maricevich M, Carlsen B, Mardini S, Moran S. Upper extremity and digital replantation. *Hand*. 2011;6(4):356-363.

40. Nishi G, Shibata Y, Tago K, Kubota M, Suzuki M. Nail regeneration in digits replanted after amputation through the distal phalanx. *J Hand Surg Am*. 1996;21(2):229-233.

41. Woo SL. Tissue engineering: Use of scaffolds for ligament and tendon healing and regeneration. *Knee Surg Sports Traumatol Arthrosc*. 2009;17(6):559-560.

42. Laurencin CT, Nair LS. The quest toward limb regeneration: A regenerative engineering approach. *Regen Biomater*. 2016;3(2):123-125.

43. Mengsteab PY, Nair LS, Laurencin CT. The past, present and future of ligament regenerative engineering. *Regen Med*. 2016;11(8):871-881.

44. Bryant SV, Gardiner DM. Regeneration: Sooner rather than later. *Int J Dev Biol*. 2018;62(6-7-8):363-368.

45. Lutolf MP, Hubbell JA. Synthetic biomaterials as instructive extracellular microenvironments for morphogenesis in tissue engineering. *Nat Biotechnol*. 2005;23(1):47-55.

46. Lu T, Li Y, Chen T. Techniques for fabrication and construction of three-dimensional scaffolds for tissue engineering. *Int J Nanomedicine*. 2013;8:337-350.

47. Iismaa SE, Kaidonis X, Nicks AM, et al. Comparative regenerative mechanisms across different mammalian tissues. *NPJ Regen Med*. 2018;3:6-018-0044-5. eCollection 2018.

48. Lehoczky JA, Tabin CJ. Lgr6 marks nail stem cells and is required for digit tip regeneration. *Proc Natl Acad Sci U S A*. 2015;112(43):13249-13254. doi: 10.1073/pnas.1518874112 [doi].

49. Takeo M, Chou WC, Sun Q, et al. Wnt activation in nail epithelium couples nail growth to digit regeneration. *Nature*. 2013;499(7457):228-232.

50. Lehoczky JA. Are fingernails are a key to unlocking the puzzle of mammalian limb regeneration? *Exp Dermatol*. 2016.

51. Montagna W. *The structure and function of skin.* Elsevier; 2012.

52. Kolarsick P, Kolarsick M, Goodwin C. Anatomy and physiology of the skin. In: .

53. Nagae H, Nakanishi H, Urano Y, Arase S. Serial cultivation of human nail matrix cells under serum-free conditions. *J Dermatol*. 1995;22(8):560-566.

54. Shi J, Lv Z, Nie M, et al. Human nail stem cells are retained but hypofunctional during aging. *J Mol Histol*. 2018;49(3):303-316.

55. Okamoto H, Kagami H, Okada K, et al. Fate of transplanted nail matrical cells and potential of hard keratin production in vivo. *J Dermatol Sci*. 2006;44(3):175-178.

56. De Berker D, Wojnarowska F, Sviland L, Westgate GE, Dawber RP, Leigh IM. Keratin expression in the normal nail unit: Markers of regional differentiation. *Br J Dermatol*. 2000;142(1):89-96.

57. Westgate G, Leigh IM. Patterns of hard keratin (ha-1) expression in nail matrix corresponds to nail plate morphology. *Br J Dermatol*. 1996;134(3):584,585.

58. Nakamura Y, Muguruma Y, Yahata T, et al. Expression of CD90 on keratinocyte stem/progenitor cells. *Br J Dermatol*. 2006;154(6):1062-1070.

59. Kitahara T, Ogawa H. Variation of differentiation in nail and bovine hoof cells. *J Invest Dermatol*. 1994;102(5):725-729.

60. Park JH, Lee DY, Jang KT, et al. CD13 is a marker for onychofibroblasts within nail matrix onychodermis: Comparison of its expression patterns in the nail unit and in the hair follicle. *J Cutan Pathol*. 2017;44(11):909-914.

61. Watt FM. Involucrin and other markers of keratinocyte terminal differentiation. *J Invest Dermatol*. 1983;81(1 Suppl):100s-3s.

62. Picardo M, Tosti A, Marchese C, et al. Characterization of cultured nail matrix cells. *J Am Acad Dermatol*. 1994;30(3):434-440.

63. Gupchup GV, Zatz JL. Structural characteristics and permeability properties of the human nail: A review. *J Cosmet Sci*. 1999;50(6):363-386.

64. Bragulla HH, Homberger DG. Structure and functions of keratin proteins in simple, stratified, keratinized and cornified epithelia. *J Anat*. 2009;214(4):516-559.

65. Gredmark S, Britt WB, Xie X, Lindbom L, Soderberg-Naucler C. Human cytomegalovirus induces inhibition of macrophage differentiation by binding to human aminopeptidase N/CD13. *J Immunol*. 2004;173(8):4897-4907.

66. Bodnar RJ. Epidermal growth factor and epidermal growth factor receptor: The yin and yang in the treatment of cutaneous wounds and cancer. *Adv Wound Care (New Rochelle)*. 2013;2(1):24-29.

67. Yamakawa S, Hayashida K. Advances in surgical applications of growth factors for wound healing. *Burns Trauma*. 2019;7:10-019-0148-1. eCollection 2019.

68. Kim HS, Yoo HS. In vitro and in vivo epidermal growth factor gene therapy for diabetic ulcers with electrospun fibrous meshes. *Acta Biomater*. 2013;9(7):7371-7380.

69. Edwards NJ, Stone R, Christy R, Zhang CK, Pollok B, Cheng X. Differentiation of adipose derived stem cells to keratinocyte-like cells on an advanced collagen wound matrix. *Tissue Cell*. 2018;53:68-75.

70. Petry L, Kippenberger S, Meissner M, et al. Directing adipose-derived stem cells into keratinocyte-like cells: Impact of medium composition and culture condition. *J Eur Acad Dermatol Venereol*. 2018;32(11):2010-2019.

71. Martins C, Sousa F, Araujo F, Sarmento B. Functionalizing PLGA and PLGA derivatives for drug delivery and tissue regeneration applications. *Adv Healthc Mater*. 2017.

72. Norouzi M, Shabani I, Ahvaz HH, Soleimani M. PLGA/gelatin hybrid nanofibrous scaffolds encapsulating EGF for skin regeneration. *J Biomed Mater Res A*. 2015;103(7):2225-2235.

73. Nguyen TH, Lee BT. The effect of cross-linking on the microstructure, mechanical properties and biocompatibility of electrospun polycaprolactone-gelatin/PLGA-gelatin/PLGA-chitosan hybrid composite. *Sci Technol Adv Mater*. 2012;13(3):035002.

74. Nguyen TH, Lee BT. The effect of cross-linking on the microstructure, mechanical properties and biocompatibility of electrospun polycaprolactone-gelatin/PLGA-gelatin/PLGA-chitosan hybrid composite. *Sci Technol Adv Mater*. 2012;13(3):035002.

75. Yu Y, Cui H, Zhang D, Liang B, Chai Y, Wen G. Human nail bed-derived decellularized scaffold regulates mesenchymal stem cells for nail plate regeneration. *J Tissue Eng Regen Med*. 2019.

76. Fernandez Canedo I, Blazquez Sanchez N, De Troya Martin M. Chemical matricectomy with phenol. *Actas Dermosifiliogr*. 2013;104(1):79-80.